WAVE INDUCED FATIGUE ASSESSMENT ON FREE SPANNING PIPELINES

Juana Waterkemper Fernandes

Dissertação de Mestrado apresentada ao Programa de Pós-Graduação em Engenharia Oceânica, COPPE, da Universidade Federal do Rio de Janeiro, como parte dos requisitos necessários à obtenção do título de Mestre em Engenharia Oceânica.

Orientadores: Bianca de Carvalho Pinheiro
Ilson Paranhos Pasqualino

Rio de Janeiro
Março de 2019

WAVE INDUCED FATIGUE ASSESSMENT ON FREE SPANNING PIPELINES

Juana Waterkemper Fernandes

DISSERTAÇÃO SUBMETIDA AO CORPO DOCENTE DO INSTITUTO ALBERTO LUIZ COIMBRA DE PÓS-GRADUAÇÃO E PESQUISA DE ENGENHARIA (COPPE) DA UNIVERSIDADE FEDERAL DO RIO DE JANEIRO COMO PARTE DOS REQUISITOS NECESSÁRIOS PARA A OBTENÇÃO DO GRAU DE MESTRE EM CIÊNCIAS EM ENGENHARIA OCEÂNICA.

Examinada por:

_____

Profª Bianca de Carvalho Pinheiro, D.Sc.

_____

Prof. Ilson Paranhos Pasqualino, D.Sc.

_____

Prof. José Luiz França Freire, Ph.D.

_____

Prof. Ney Roitman, D.Sc.

RIO DE JANEIRO, RJ – BRASIL

MARÇO DE 2019

Fernandes, Juana Waterkemper

Wave Induced Fatigue Assessment on Free Spanning Pipelines/ Juana Waterkemper Fernandes. – Rio de Janeiro: UFRJ/COPPE, 2019.

XII, 75p.: il.; 29,7 cm.

Orientadores: Bianca de Carvalho Pinheiro

Ilson Paranhos Pasqualino

Dissertação (Mestrado) – UFRJ/ COPPE/ Programa de Engenharia Oceânica, 2019.

Referências Bibliográficas: p. 71-73.

1. Pipeline. 2. Scour. 3. Fatigue 4. Pipe-Soil Interaction. I. Pinheiro, Bianca de Carvalho *et al*. II. Universidade Federal do Rio de Janeiro, COPPE, Programa de Engenharia Oceânica. III. Título.

AGRADECIMENTOS

Primeiramente aos meus pais, Celso e Marli, por sempre me incentivarem a buscar excelência em todos os meus trabalhos e por terem me apoiado de todas as formas possíveis durante o mestrado. Sem eles, seria impossível conseguir concluir este curso.

Aos meus irmãos, Mariana e Mauro Henrique pelo apoio. Aos meus sobrinhos Augusto e Henrique, que alegram todos os meus dias, mesmo que de longe. E ao meu sobrinho Pedro (*in memorian*), meu anjinho da guarda.

Ao meu amigo e namorado, Fernando, por me aguentar reclamando durante esse tempo todo.

À minha orientadora, Bianca, por ter acreditado no meu trabalho e me ajudado nesse processo. Aos professores do LTS e funcionários do LTS, em especial à Cris por ter me ajudado em momentos difíceis e ao Zé Carlos por todos os (muito necessários) cafezinhos.

Aos amigos que fiz no mestrado, que sempre se esforçaram para serem pessoas presentes e por me ajudarem a me adaptar aqui no Rio de Janeiro.

Ao Irving e Marcelo pela ajuda na obtenção e tratamento dos dados de onda.

Ao Conselho Nacional de Desenvolvimento Científico e Tecnológico – CNPq, pela bolsa de mestrado.

Resumo da Dissertação apresentada à COPPE/UFRJ como parte dos requisitos necessários para a obtenção do grau de Mestre em Ciências (M.Sc.)

AVALIAÇÃO DE FADIGA INDUZIDA POR ONDAS EM PIPELINES APRESENTANDO VÃO LIVRE

Juana Waterkemper Fernandes

Março/2019

Orientadores: Bianca de Carvalho Pinheiro
Ilson Paranhos Pasqualino
Programa: Engenharia Oceânica

Sabe-se que inspeções geofísicas e batimétricas devem ser feitas durante a etapa de definição da rota de um pipeline para que vãos livres sejam evitados, já que este tipo de configuração pode levar a estrutura à instabilidade quando associada aos fenômenos de vibração induzida por vórtices (VIV) e ação diretas das ondas. No entanto, vãos livres também podem ser formados durante a fase de operação, devido ao processo de *scour* ou liquefação. Com as mudanças climáticas recentes, fenômenos como furacões e ciclones estão se tornando cada vez mais frequentes, chamando atenção para ameaças vindas de ondas e correntes extremas sobre estruturas oceânicas como os *pipelines*.

Neste trabalho, um modelo numérico tridimensional é desenvolvido usando o método dos elementos finitos (MEF) com o auxílio o software ABAQUS, compreendendo um duto modelado com elementos de casca e um leito marinho representado por um sólido contínuo. A interação através do contato entre as duas partes também é considerada.

Por fim, este trabalho apresenta resultados de um amplo estudo paramétrico variando o tamanho do vão livre, o diâmetro do *pipeline*, o estado de mar e o solo, cujas sensibilidades em relação à vida em fadiga são analisadas. Essa pesquisa toma os resultados numéricos para o cálculo do dano de fadiga no duto com vão livre devido a ondas diretas, em águas intermediárias, com base em recomendações da DNV referentes ao caso em análise.

Abstract of Dissertation presented to COPPE/UFRJ as a partial fulfillment of the requirements for the degree of Master of Science (M.Sc.)

WAVE INDUCED FATIGUE ASSESSMENT ON FREE SPANNING PIPELINES

Juana Waterkemper Fernandes

March 2019

Advisors: Bianca de Carvalho Pinheiro
Ilson Paranhos Pasqualino

Department: Ocean Engineering

It is well known that geophysical and geotechnical surveys must be performed in a pipeline route to avoid free spans, since this configuration could bring the structural integrity to jeopardy concerning the fatigue behavior, associated with both vortex induced vibration (VIV) or direct waves actions. However, free spans can be formed during the operation phase due to scour or liquefaction processes. With the recent world's climate changes, phenomena such as hurricanes and extreme storms are becoming more frequent, raising the awareness of the threat from wave loads on offshore structures, such as pipelines.

In this work, a three-dimensional numerical model, based on the finite element method (FEM), is developed, with ABAQUS, comprising a pipe modeled with shell elements and a seabed represented by solid elements, and taking into consideration the contact between these two parts.

Finally, the work gathers and presents information of 96 analysis, displaying a parametric study that varies the span length, the diameter, the sea state and soil, that is useful to find the sensitivity of each parameter. This thesis applies the results given by the FEM model to evaluate the accumulated fatigue damage in free spanning pipelines due to the action of direct waves, within intermediate waters, considering and briefly commenting some of DNV's recommended design practices available for this case.

CONTENT

Figure Content

Table Content

Nomenclature

L – Span length

L_{sh}– Span shoulder

L_w – Wave length

h – Water Depth

α – Wave coefficient

U_C– Magnitude of current velocity

U_w– Magnitude of wave velocity

e – Span gap

ε– Strain/deformation

Ψ – Dilatancy angle

Φ – Friction angle

E – Young modulus

Δσ – Stress range

υ - Poisson ratio

H_s – Significant wave height

T_p – Peak period

σ_e – Proportional limit

σ_y – Yield strength

σ_a – Stress amplitude

σ_m – Mean stress

S_f – Fatigue limit for a completely reversed load

S_u – Ultimate tensile strength

1. Introduction

Even though fairly researched, the soil structure interaction (SSI) that happens during a wave passing over a structure laid in the marine bed is still one of the challenges in subsea pipelines design. It is known that the flow around these structures has a high erosive potential and it can cause a number of structural problems to the pipelines. For instance, when there is erosion around a pipe exposed to waves, it loses its support and gets mechanically challenged, possibly leading to failure.

Fatigue is one the most common failure modes for this subject, due to the presence of intermittent varying loads in the oceans, such as waves and currents, the VIV (*Vortex Induced Vibrations*) is particularly concerning in this issue, because of both wave and current loads and their flow. One configuration resulting from seabed dynamics, that is especially affected by waves due to the lack of foundation support, will be the focus of the present work.

The United Nations Office for Disaster Risk Reduction released a report on the number of natural disasters reported per country in a time span of 20 years, Fig. 1, where it is noticeable that USA, China and Brazil have had a high number of disasters.

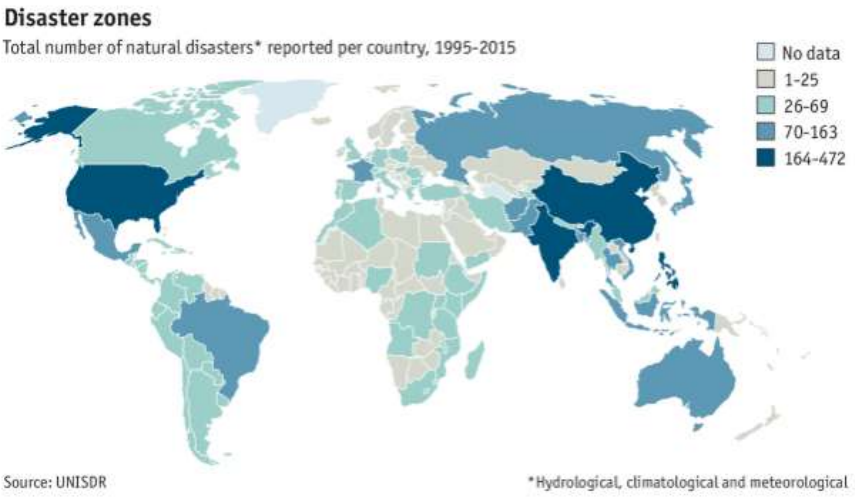

Figure 1 - World Natural Disaster Distribution [1]

Also, in the past 36 years, the occurrence of natural disasters such as storms, hurricanes and floods has skyrocketed, and an analysis provided by an insurance group, Munich Re, has indicated that the trend is bound to continue the same way or even worse (Fig. 2).

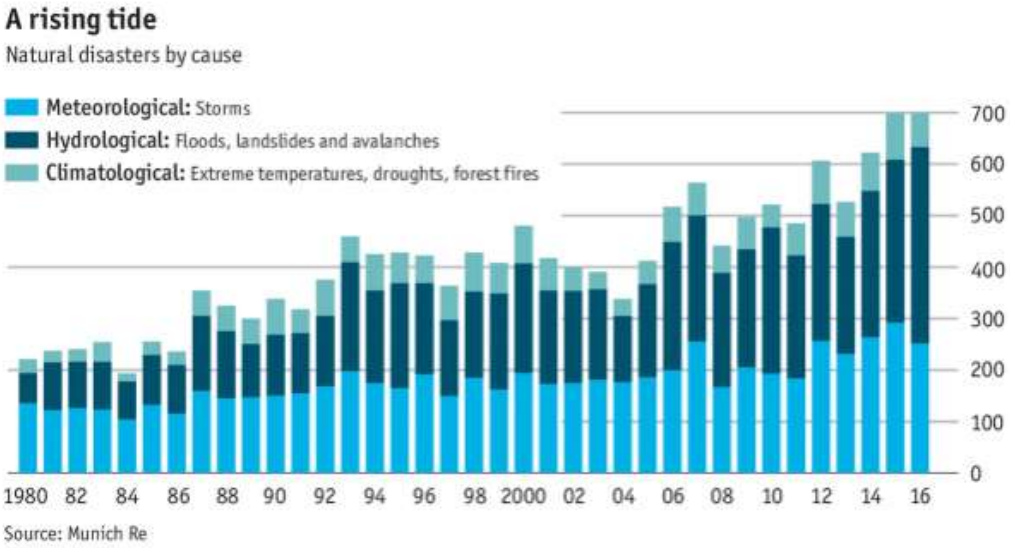

Figure 2 – Distribution of Europe's Natural Disasters by Year [2]

Meteorological events have a great influence on the sea state, meaning that waves can reach unprecedent heights and frequencies, which can be extremely damaging to offshore and coastal structures.

Hydrocarbons make up for more than half of the world's energy matrix, as seen in Fig. 3, being that way, researches to reduce installation costs and to improve safety are in continuous development. In the case of free spanning pipelines, the interests are economic and environmental.

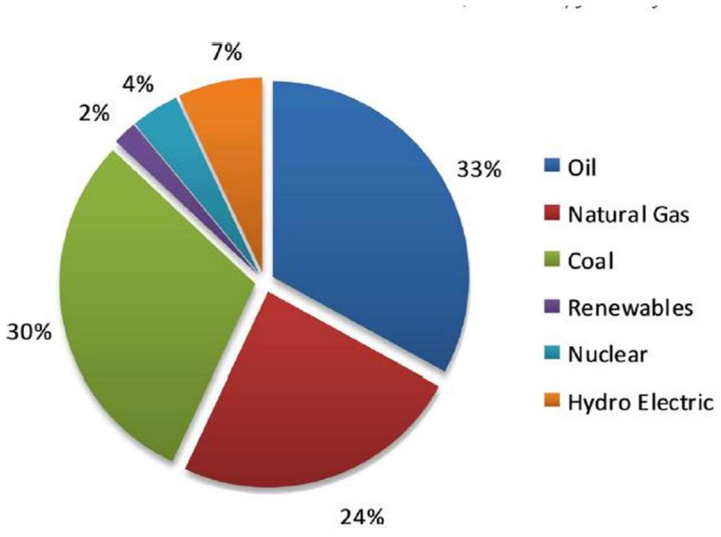

Figure 3 - Global Energy Matrix Estimative [3]

The economic value spent today with mitigation is still high and not always effective, according to Pulse Monitoring [4]. Free spans are not completely understood when it comes about its interaction with the marine bed, which leads to a great level of uncertainties that are usually corrected with highly conservative methods that can be quite expensive.

Shore-end pipelines or marine outfalls pipes are among the structures that suffer the most, Fig. 4, because of the seabed scouring dynamics that can deprive the pipes out of structural support, leading to a free-spanning pipeline configuration.

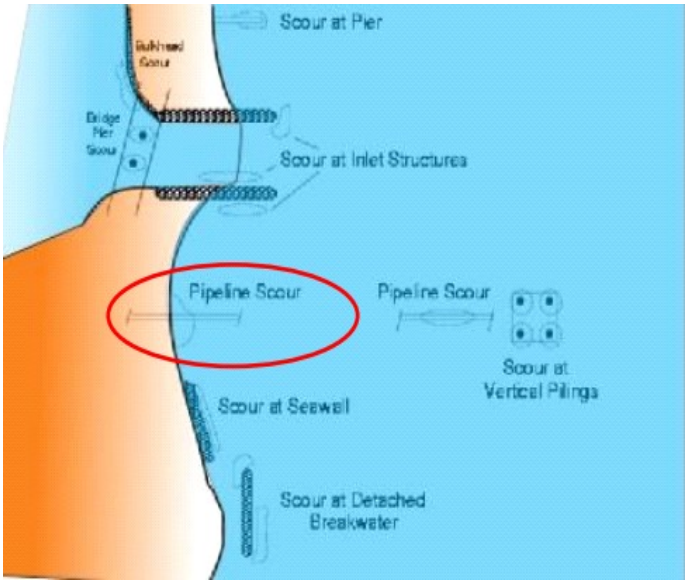

Figure 4 - US Marines Coastal Protection [5]

This work aims to study the response of free-spanning pipelines under extreme wave inertia loads in the in-line direction – that are often disregarded. In this document, a brief review of the DNV recommended practices for free spanning pipelines and soil-structure interaction is made and used as guidance to a parametric study that longs to identify the sensitivity of parameters such as soil, sea state and span length in the fatigue life reduction of a steel pipeline.

Then, a three-dimensional model is proposed to perform a parametric study, with the seabed modeled as a solid and the pipe modeled as a thin shell, varying the diameter of the pipe, the span length, the soil type and the sea state. The results of the parametric study are, then, used in a fatigue analysis study.

For this type of problem, two-dimensional analyses are widely applied due to its simplicity and reliability, though they often disregard the plastic behavior of the soil and, therefore, the proper pipe-soil interaction. Then, the aim of using a three-dimensional model is to analyze

how parameters that are often disregarded in two-dimensional analyses may affect the structural response of free spanning pipelines.

2. Literature Review

In this section, some terms and phenomena are briefly described for a better understanding of this work, as well as some pertinent advances in soil structure interaction (SSI) studies and free spanning pipelines.

Scouring phenomena such as liquefaction of the soils and sediment transport are explained, with some examples of different ways they act upon the structure and some previously reported cases.

In addition, the two recommended practices followed in this work, DNV-RP-F105 – for free spanning pipelines – and DNV-RP-F114 – for pipe-soil interaction –, are partially assessed to guide this work in pertinent issues.

In addition, mitigation processes and some of its recourses available in the market are explained taking in consideration the effectivity when dealing with the scouring phenomenon.

2.1 Free Spanning Pipelines – Definition & Formation

Free spans are characterized by a length of pipeline without any type of structural support. They can be formed due to preexistent conditions of the marine bed or due to a diversity of dynamic interactions that happens in the seabed.

Two of the most common applications of rigid pipelines are hydrocarbons pipelines and marine outfalls. In this section, the main types of span formation for these two types are briefly explained.

2.1.1 Irregular Bathymetry

During the pipeline route specification, the local bathymetry is analyzed – as shown in Fig. 5 - and sometimes, depending on how troubled the soil surface is, the simply laying of the pipe will result in free spans. Although this does not represent ‘free span formation’, an analysis should be performed to define if the instantaneous spans are harmless to the structure or if mitigation procedures should be applied.

According to the DNV-RP-F105, a first assessment of the free spans along the pipeline route should contain, at least:

- span length/gap measured and well defined due to span supports or uneven seabed;
- soil properties assessed by soil samples along route;
- site-specific long-term distributions of environmental data available;

- test on effect of changes in operational conditions.

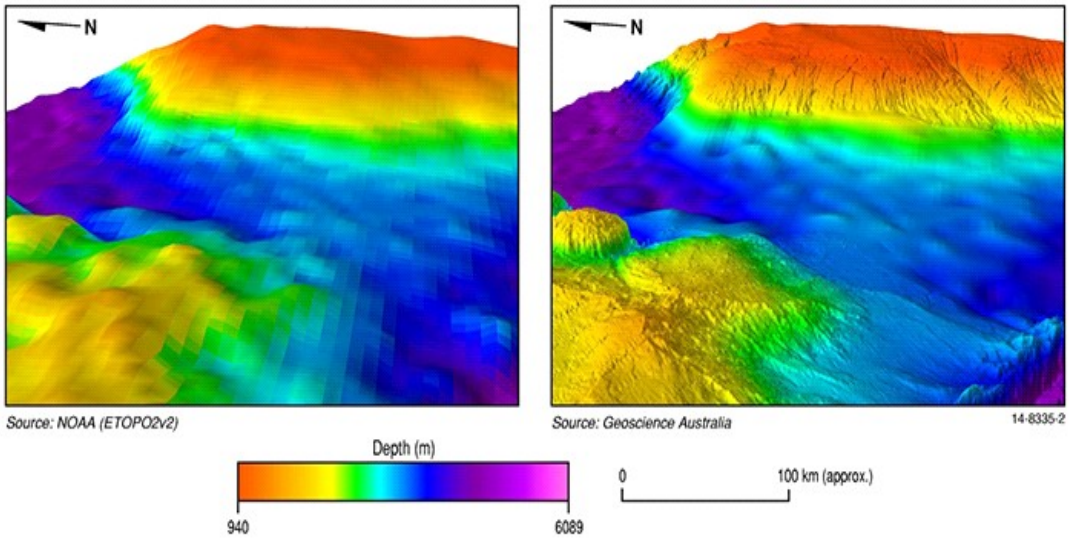

Figure 5 - Example of Bathymetry Results [6]

A common example of preexistent conditions of the seabed are pockmarks, that are geological depressions in the seabed caused by gasses and/or liquids that erupt and stream through the sediments. The width of pockmarks ranges between 3 m to over 700 m, with depths varying from centimeters to over 15 meters. A large pockmark example can be seen in Fig. 6.

When they are identified in the bathymetry results, the first thing to consider is to change the pipeline route, but it is not always possible. Then, analysis should be performed to identify if the pockmarks will cause free spanning pipelines within the permissible lengths giving by the recommended practices. If they are not within the safe range of spans, mitigation procedures should take place.

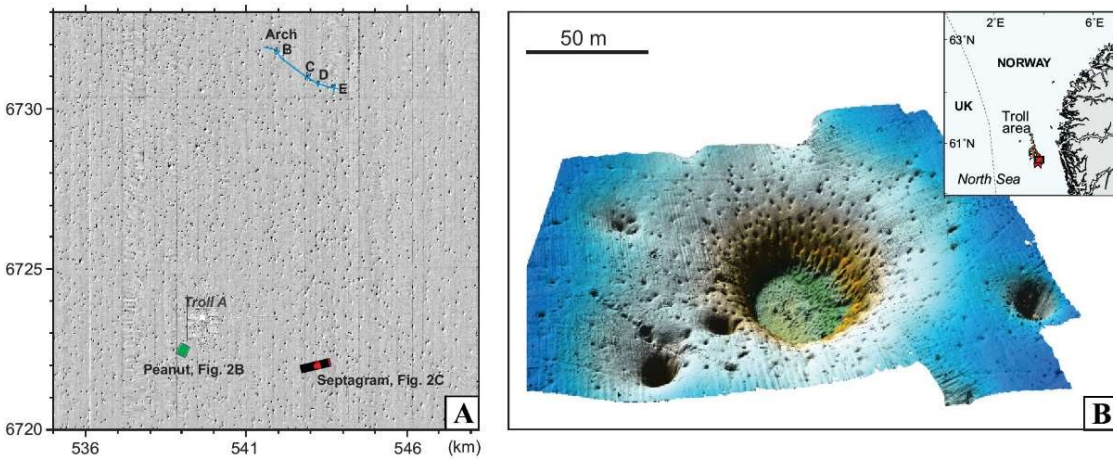

Figure 6 - Parts of the Troll Pockmark Field off Norway. A: Density of Pockmarks in an Area of 169 Aquare km. B: Details of a Cluster of Pockmarks [7]

2.1.2 Pipeline laid over permafrost

Restricted to extremely cold environments, a free span condition might arise from a pipeline laid over permafrost, this configuration occurs when the bathymetry results do not accuse the permafrost presence; it can be hidden down in a layer of soil, as Fig. 7, for example.

Composed of soil, rock (pebbles or grave) and ice, the permafrost can have a water percentual over 30% [8]. In this case, when the pipeline is laid during the winter, the outcome can be problematic – the heating of the waters in the summer can melt the permafrost, leaving a span right below the pipeline. This problem is commonly known as permafrost thaw.

Figure 7 - Melting Permafrost in Norway [8]

In 2013, *PEW Center* researches released an 'Artic Oil Spill Prevention Manual' [9]. For a pipeline over permafrost case, Fig. 8, the prevention recommendations included: random sampling of the soil, continuous in-line inspection and, if possible, a thicker-walled pipe.

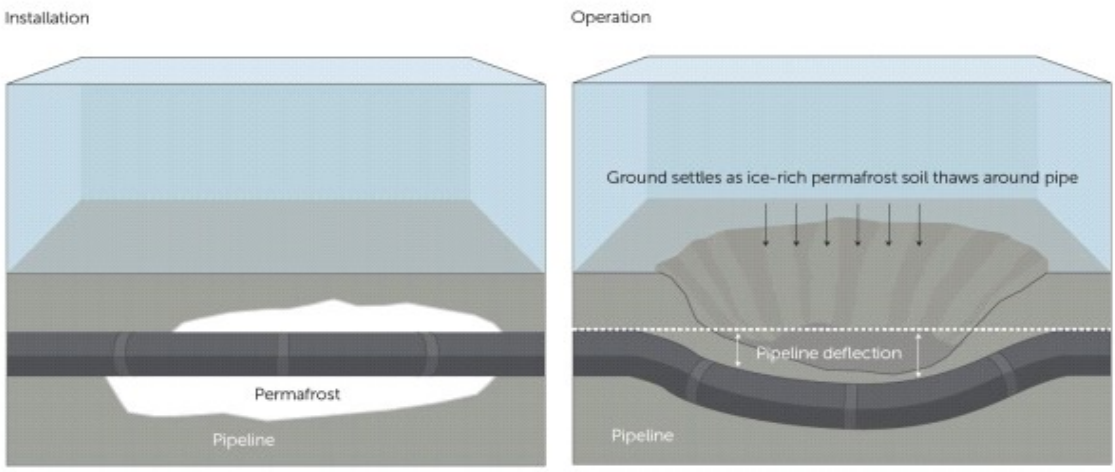

Figure 8 - Pipeline over Permafrost [9]

2.1.3 Scour

According to Hughes [10], scour is the removal, through hydrodynamic forces, of the granular material of the marine bed nearby marine structures, and it is usually present in nearshore sites, where the waves and currents dynamics have a great influence over the seabed, Fig. 9.

It can be described as a particular form of the erosion phenomenon and it is, potentially, the most critical case of free spans formation. The susceptibility to scouring of the seabed depends mostly of the wave climate of a region, along with the sediment size.

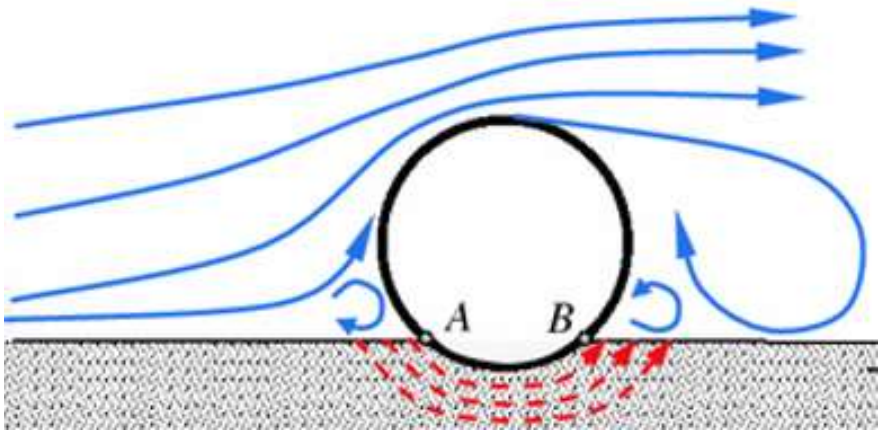

Figure 9 - Scour Dynamics. Adapted from [11]

Scouring has two main mechanisms: liquefaction and sediment transport, both are dependent on the size of the grain. For instance, as seen in Fig. 10, only small diameters

sediments are susceptible to liquefaction and that should be the first thing to be defined in the project: whether or not the seabed soil has a risk of liquefaction. Then, the different mechanisms can be assessed, and, if the Met Ocean data is available, the scour can be predicted.

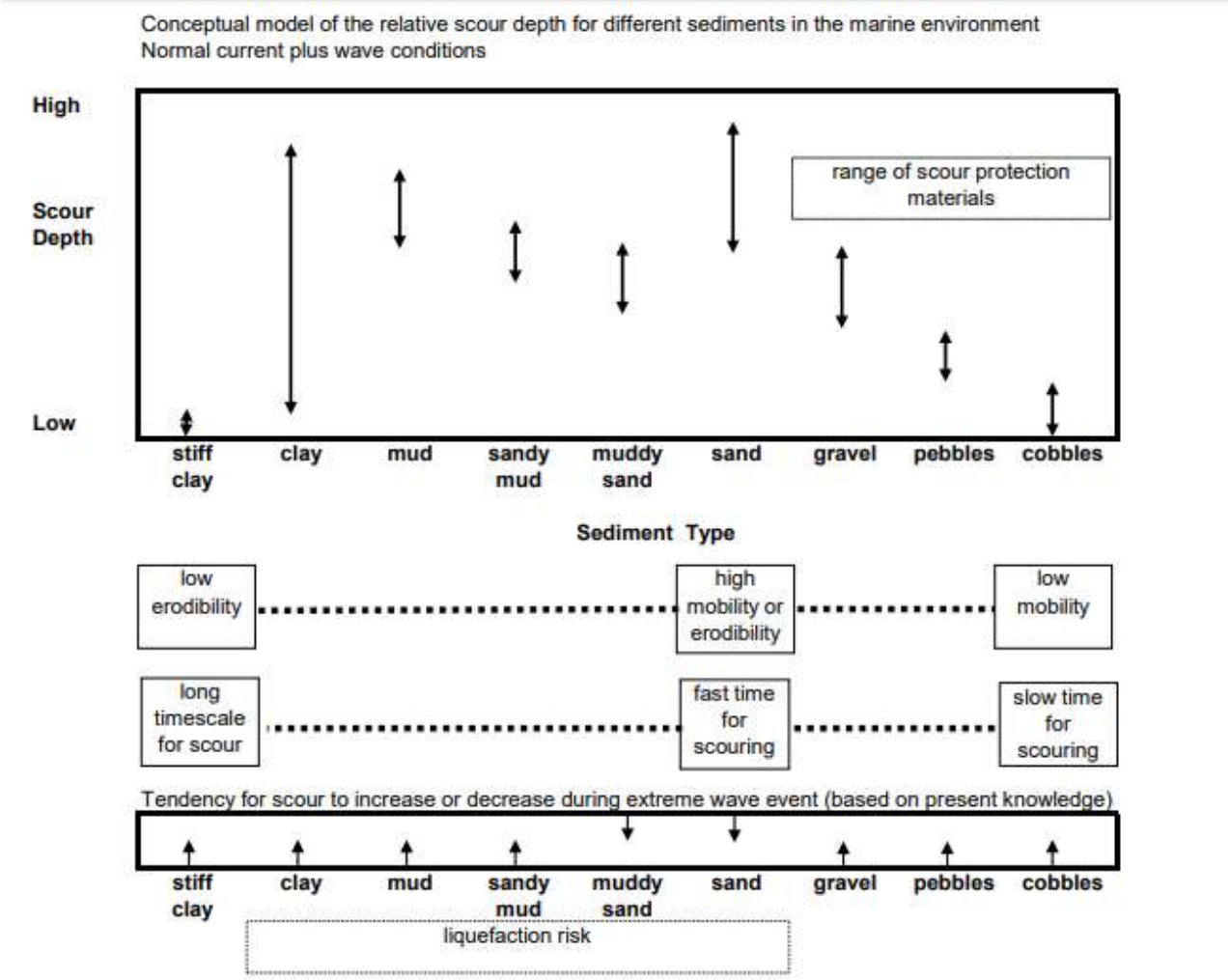

Figure 10 - Scour Predictability [12]

The most complicated cases of scouring for engineering purposes are related to soils with less cohesion among the grains, as can be seen in Fig. 10, where mostly higher scour depths can be found in sand. Moreover, scouring in certain types of sand usually has a “fast time occurrence”, With their mobility and erodibility being considerably bigger than clays and muds. It means that, given an exposed pipeline, it could take only a few hours under wave action to form a free-span. And that is the reason why mixing any other material to the pipeline trench, except clay, can help retard the erodibility of the sand.

2.1.3.1 Liquefaction

According to Sumer [13], Marine soils are continually exposed to wave action. The liquefaction phenomenon is essentially linked with large waves. These waves may have a period of the magnitude order between 5 and 15s, with 50 and 100-year-return-period wave heights, as much as 1 to 2 m or larger in coastal areas and 10 to 20 m in offshore areas.

Liquefaction is generated mainly by two different mechanisms, namely:

1. Buildup of pore pressure (residual liquefaction); and
2. Upward-directed vertical pressure gradient in the soil during the passage of a wave trough (momentary liquefaction).

Cohesive soils, such as clays and silts, are prone to liquefaction. A long period exposed to wave action can make the soil lose the cohesion between the grains, resulting in pore pressure excess, which will make the soil experience a loss of tension among its grains and behave as a fluid admixture, offering no proper support to whichever structure laid on or onto them. The whole process can be visualized in Fig. 11.

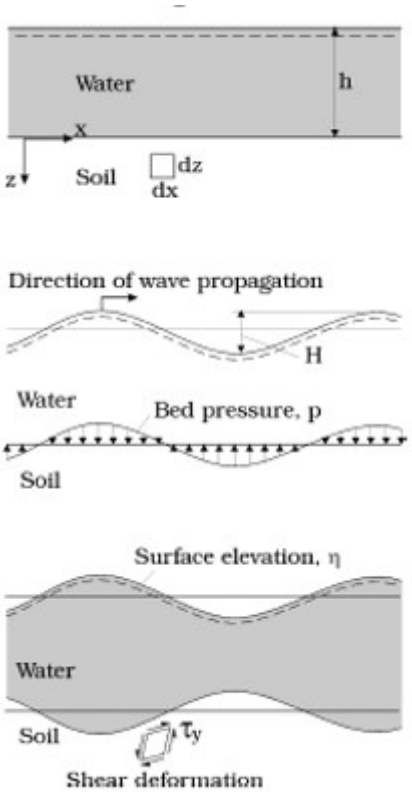

Figure 11 - Cohesive Soil Mechanism. Adapted from [13]

Depending on what the pipeline is transporting, that might result in floating, sinking or lateral displacement (Fig. 12). Even when the pipeline is buried, if there was liquefaction, a virtual free span formation can be formed.

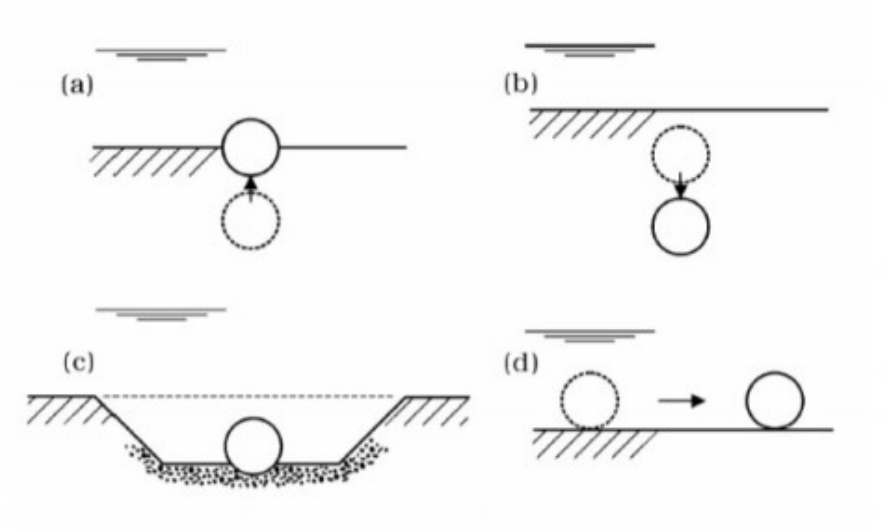

Figure 12 - (a) Pipeline floating; (b) Pipeline sinking; (c) Rock cover sinking; (d) Lateral Displacement of the pipeline [13]

A very astonishing case can be observed in Fig. 13, where a pipeline was laterally displaced after a storm in Shat Al-Arab delta, near Fao Islands. According to Summer [13], the pipeline was installed in a pre-dredged trench by a bottom pull operation. The seabed material was described as "very soft sandy silt". Due to waves and tidal motion the seabed soil around the trench turned into a dense liquid that flooded the trench and, as a result, the pipe floated.

Figure 13 - Lateral Displacement of a Pipeline after a Storm. [13]

2.1.3.2 Sediment Transport

Van Rijin [14] explained sediment transport - more specifically sand transport - as the relocation of particles with size between 0.05 mm and 2 mm, driven by waves and/or currents. This mechanism is not always reliable when described computationally, so researchers usually rely on field experiments or reduced scale physical models to get answers.

For a particle to move, the hydrodynamic bottom shear stress must be larger than the sediment critical shear stress, and there are two main phase specifications in sediment transport, bed load and suspended load, Fig. 14.

Bed load can be defined as the starting movement of the grains, when they receive the necessary energy to move. Suspended load, otherwise, is a type of transport linked to turbulent flows. Summing up, the suspended load can generate erosion in a short term, few minutes, while the bed load can take days. They are also called live bed scour and clear water scour, respectively.

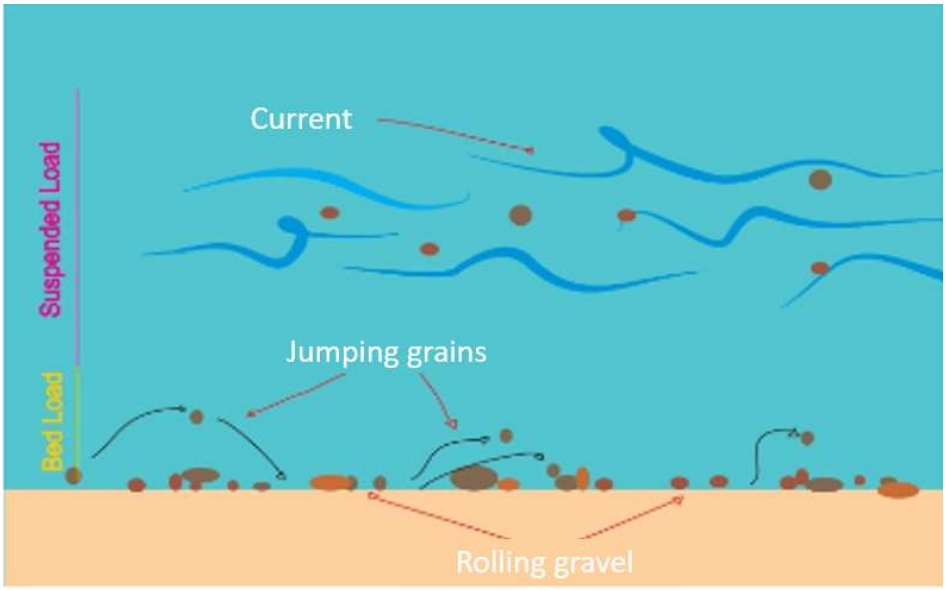

Figure 14 - Sediment Transport. [15]

In 2015, an experimental study was carried out in a fluid-structure interaction laboratory to demonstrate the erosive potential of waves over simply-laid pipelines and semi-buried pipelines, Fig. 15. The experiment based its set-up, shown in Fig. 16, in a paper by Sumer [16] that evaluated build-up pressure in the soil during wave passing.

Figure 15 - Reproduction of [16] Experiment with Pipelines: (b) Initial Setup; (c) After 15 minutes of Progressive Waves [17]

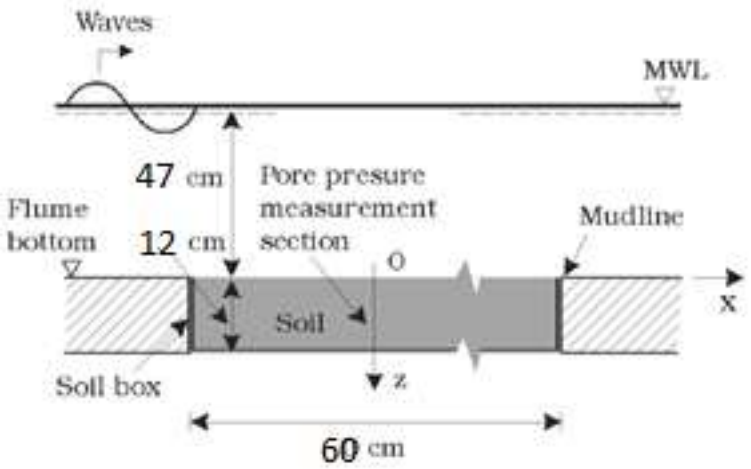

Figure 16 - Experimental Set up. Adapted [16]

That experiment, Fig. 16, was a starting point to this current work. In it, the erosive potential of the waves could be observed in different combinations of wave frequencies and water depth, but at the time, the structural part of it was not up for analysis, as it was a sediment transport experiment only.

Still within the sediment transport issue, some special phenomena can be observed in nature. The strudel scour, Fig. 17 occurs in cold zones and during the spring melt, when a large volume of freshwater flows into a pack of ice and drains through a hole or a crack in the ice, creating a severe whirlpool down to the seabed. This way, the water pressures the soil and can results in a hole over 4 m deep.

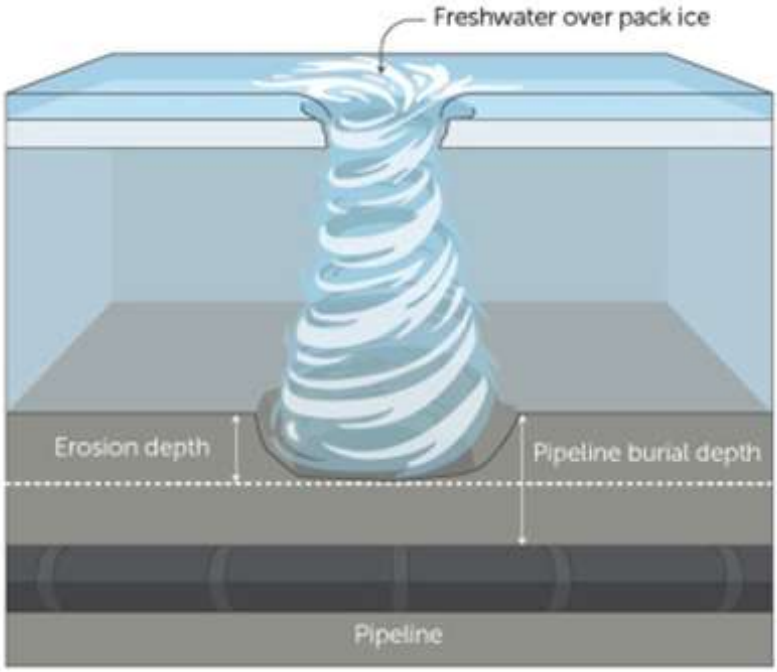

Figure 17 – Strudel Scour in Action [9]

2.2 Recommended Practices

One of the most widely accepted recommended practices and classifications for offshore structures, are issued by Det Norske Veritas – DNV. In this work, some recommended practices items by DNV are followed and applied during the model implementation and result analysis.

2.2.1 DNV-RP-F105 – Free Spanning Pipelines

According to DNV "This recommended practice considers free spanning pipelines subjected to combined wave and current loading. The premises for the document are based on technical development within pipeline free span technology in research and development (R&D) projects, as well as design experience from previous projects and the basic principles applied in this document agree with most recognized standards and reflect state-of-the-art industry practice and latest research and ongoing projects."

In this section some points of the DNV-RP-F105 - the ones used as guidance to the present work - are briefly reviewed.

2.2.1.1 Morphological Classification of Free Spans

Free span morphological classification is usually taken as starting point to define different parameters and possible analysis scenarios, as well as distinguish between isolated and interacting free spans. Essentially, the free spanning pipelines have three main features: the span length, the span shoulders and the span depth, all illustrated in Fig. 18, and explained below according with the DNV-RP-F-105 standard [17].

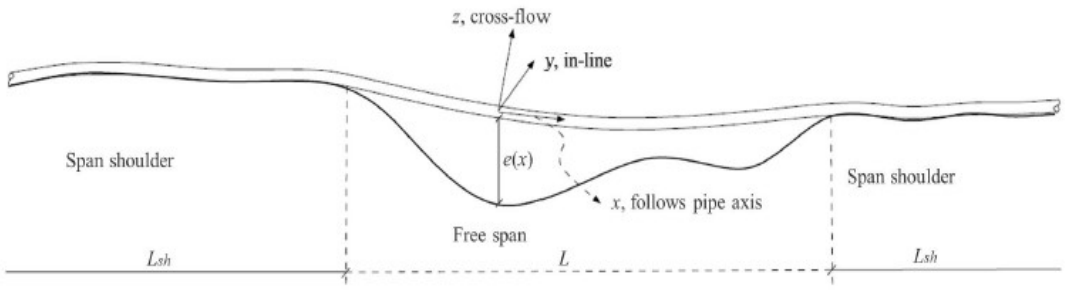

Figure 18 – Elements of a Free Spanning Pipeline [17]

The span length, L, is commonly known as the free span size, and it is characterized by a section of the pipe with no seabed support whatsoever. The span shoulder, L_{sh}, is characterized by a section of pipe-soil contact. The span depth, e(x), is the orthogonal distance between the lower portion of the pipe to the scoured seabed surface.

If a free span is disconnected from other spans by considerable stretches of pipe-soil contact, it can be considered an isolated single span. Nevertheless, in typical uneven seabed configurations, spans are often in immediacy. A qualitative description of the distinction between isolated single spans and interacting multi-spans is given as follows:

- A free span is an isolated single span if the static and dynamic behavior are negligibly affected by neighboring spans, if any;
- An arrangement of two or more spans is an interacting multi-span if the static and dynamic behaviors of the spans are affected by other spans in the sequence.

In this work, due to its simplicity to analyze and compatibility with the computational resources available, a single span was defined as the study case.

2.2.1.2 Free Spans Response

An overview of typical free span characteristics is given in Table 1, as a function of the free span length and the pipeline diameter, the ranges indicated for the normalized free span length are given in terms of (L/D).

Table 1 - Free Spanning Response Behavior [17]

L/D	*Response description*
$L/D < 30$ [1)]	**Very little dynamic amplification** Normally not required to perform comprehensive fatigue design check. Insignificant dynamic response from environmental loads expected and unlikely to experience VIV. Natural frequency sensitive to soil stiffness. Due to high modal stresses, onset criteria for VIV recommended.
$30 < L/D < 100$	**Response dominated by beam behaviour** Relevant for free spans at uneven seabed. Natural frequencies are sensitive to boundary conditions, effective axial force (including initial deflection, geometric stiffness) and pipe feed in.
$100 < L/D < 200$	**Response dominated by combined beam and cable behaviour** Relevant for free spans at uneven seabed in temporary conditions. Natural frequencies sensitive to boundary conditions, effective axial force (including initial deflection, geometric stiffness) and pipe "feed in". See [1.7] for free span response classification, which provides practical guidance for engineering applications, with respect to single and multi-mode response.
$L/D > 200$	**Response dominated by cable behaviour** Relevant for small diameter pipes, or pipes exposed to mild environmental conditions, typically in deep water. Natural frequencies governed by deflected shape, span interaction and effective axial force.
1) For hot pipelines (response dominated by the effective axial force) or under extreme current conditions (U_c > 1.0 – 2.0 m/s) this L/D limit may be misleading.	

This work sets the beam behavior, since it is more easily modelled and can occur often during the operation phase [17].

2.2.1.2 Flow Regimes

When analyzing the susceptibility of certain phenomena, defining what kinds of issues are present in a pipeline laying location should be one of the first steps. Here are how the flow regimes are classified by the DNV, based on equation 1.

$$\alpha = \frac{U_c}{U_c + U_w} \tag{1}$$

Where,

α – Wave coefficient

U_C– Magnitude of current velocity

U_w– Magnitude of wave velocity

The flow regimes can be further classified according to in-line or cross-flow directions.

- Wave dominant – Wave superimposed by current ($\alpha < 0.5$)

In-line direction: in-line loads can be described according to Morison's equations [17]. In-line VIV due to vortex shedding is negligible.

Cross-flow direction: loads are mainly due to asymmetric vortex shedding.

- Wave dominant – Current Superimposed by wave ($0.5 < \alpha < 0.8$)

In-line direction: in-line loads can be described according to Morison's equations. VIV due to vortex shedding is reduced due to the presence of waves.

Cross-flow direction: loads are mainly due to asymmetric vortex shedding and resemble the current dominated situation.

- Current dominant ($\alpha > 0.8$)

In-line direction: A steady drag dominated component and an oscillatory component due to regular vortex shedding.

Cross-flow direction: loads are cyclic and due to vortex shedding, resembling the current dominated situation.

2.2.1.3 Boundary Conditions

As can be read in the DNV-RP-F105 "The boundary conditions applied at the ends of the modelled pipeline section shall adequately represent the pipe-soil interaction and the continuity of the pipeline. Enough lengths of the pipeline at both sides of the span shall be included in the model to account for the effects of side spans, if relevant."

The recommended practice also states that "The boundary conditions for free span analysis can be represented with different sophistication levels. The fitting choice for boundary conditions will depend on the purpose of the free span analysis and the uncertainty of relevant input parameters, such as environmental loads, soil properties, and seabed topography."

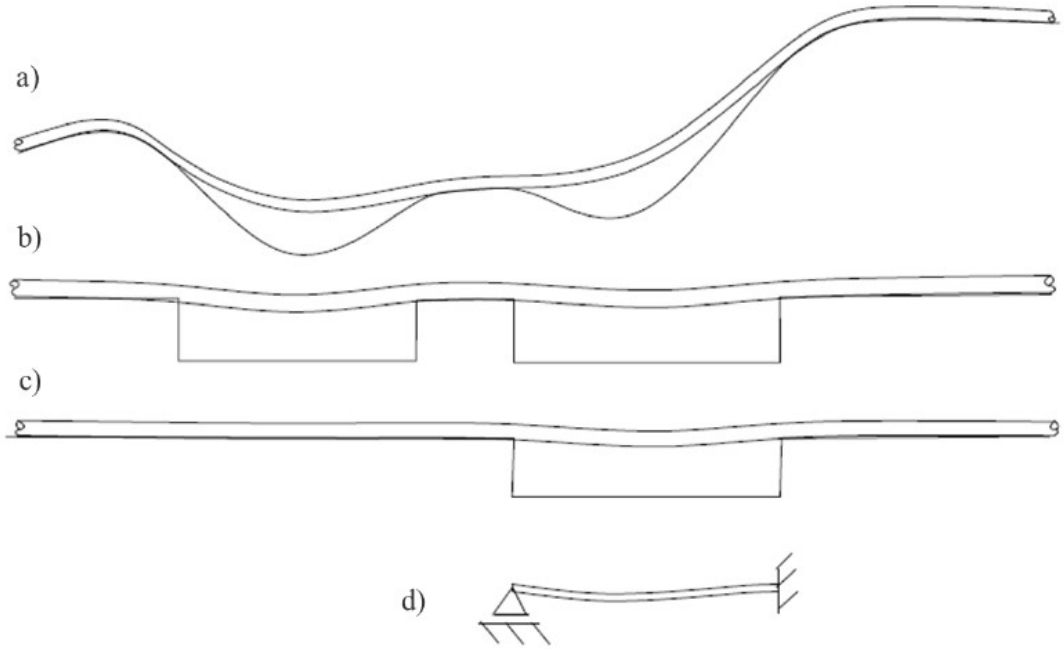

Figure 19 – a) Multi-span with Realistic Seabed Model, b) Multi-span with Flat Shoulders and Intermediate Shoulder, c) Single Span with Flat Shoulders, d) Idealized Rigid Body Constraints [17]

The different free span boundary conditions, shown in Fig. 19, can be classified by [17] as:

a) Realistic seabed model, with seabed topography and all relevant side spans included in the model. A realistic seabed model is also the only boundary condition representation that can be used if the static analysis is intended to predict span lengths and gaps;
b) Flat seabed model with interacting multi-spans, where the seabed topography is disregarded, but all relevant side spans are included.
c) Flat seabed local model of isolated single-span; If accurate estimates for span lengths, gaps and effective axial forces are *a priori* available, and the span shoulders are relatively flat, a flat seabed model may be appropriate.
d) idealized rigid-body constraints, such as pinned-fixed ends. Idealized rigid-body constraints may be convenient for manual calculations and illustration of physical aspects but will generally give quite crude estimates of the pipe response.

Idealized rigid-body constraints may be used for illustration of physical aspects but are normally associated with quite crude estimates of the pipe response. The use of such boundary conditions is therefore discouraged for quantitative free span assessments.

Seabed unevenness have a significant influence on static curvatures, axial forces and bending moments. They should be included in the analysis for an accurate estimation of the

static and dynamic response quantities. A realistic seabed model is recommended, even though it is more time consuming, and shall be applied in compliance with pipe-soil interaction modelling, present in the DNVGL-RP-F114. This study uses a single span with a realistic seabed, a combination between cases a) and c) from Fig. 19.

2.2.2 DNV-RP-F114 – Pipe-Soil Interaction for Submarine Pipelines

Pipe-soil interaction is an important aspect of the pipeline project that can guarantee structural behavior and integrity of the pipeline during installation and operation. Familiarity with the soil conditions along the pipeline route is crucial to evaluate the pipe-soil interaction, and the preparation of soil investigations should be suitable for the conditions that might occur during the operation phase of the pipeline. Soil variability is inevitable over large distances and, because of the dynamics of the seabed, more occurring in the surface layers of the soil.

During installation of an exposed pipeline, the soil around the pipe will be disturbed, affecting both its strength and stiffness properties, as well as the seabed configuration close to the pipe. These installation effects are difficult to predict, as they are highly governed by the pipe motions during laying. For buried pipelines, the state of the backfilled material is challenging to predict [18].

The complexity and uncertainty in pipe-soil interaction are significant and require simplifications and assumptions in the engineering models. The effort spent on pipe-soil interaction should however reflect the sensitivity of the pipeline design.

2.2.2.1 Finite Element Methods

If pipe-soil interaction is evaluated using finite element analysis, one should thoroughly evaluate possible sources of errors and their effects on the results. The following issues are of crucial interest in this context:

- the constitutive soil model should represent the soil behavior needed for the problem at hand;
- the iteration procedure should not result in an overshoot of failure loads;
- the mesh should be sufficiently fine with proper width/length/height ratios of the elements to ensure a proper load distribution throughout the soil.

When establishing a FE model, several assumptions need to be made. The influence of the model assumptions should be investigated and evaluated. The model assumptions include the representation of the pipe, loading conditions, soil behavior and soil parameters.

2.2.2.2 Pipe Response

Pipe-soil interaction is a key element in the assessment of exposed pipelines. Typical scenarios involving pipe-soil interaction are lateral buckling, end expansion, pipeline walking, flow line anchoring, on-bottom instability, trawl impact and development of free spans. The main structural response is controlled by soil conditions, that can be checked in Table 2.

Table 2 - Pipe Soil Contact Description [18]

Response	*Description*	
Embedment (see [4.2])	The initial embedment is controlled by the soil conditions and the loads during and following installation. It has a significant influence on the subsequent axial and lateral response.	
Axial friction (see [4.3])	Axial breakout response	An initial peak in resistance that is mainly relevant to the first load response
	Axial residual resistance	The large displacement response as the pipe expands or contracts
	Cyclic axial response	The long term cyclic response under repeated expansion and contraction
Lateral resistance (see [4.4])	Lateral breakout response	An initial peak in resistance as the pipe first displaces from the as-installed position
	Lateral residual resistance	The large displacement resistance
	Cyclic lateral response	The long term cyclic response, when the pipe becomes embedded in a trench within a buckled pipe section and soil berms grow causing a rise in lateral resistance
Soil stiffness (see [4.5])	Vertical stiffness	Static and dynamic stiffness
	Lateral stiffness	Static and dynamic stiffness
Soil damping (see [4.6])	Soil damping may be introduced in dynamic analyses.	

2.3 Fatigue Problems in Free Spanning Pipelines and Mitigation

Problems involving fatigue in free spanning pipelines can be many, especially when it comes about the ones caused by waves, since, as explained before, events of harsh wave attacks can erode the seabed in a few minutes, so even if the pipeline was buried, it isn't off the risk. In coastal areas, the problems due to waves can be exceptionally big for the environment, if a working pipeline fails due to the cyclic attack of waves, the area can help a leakage spread along a large area very rapidly.

In offshore areas, besides the potential damage for the environment, it is worth mentioning the difficulty of repairing damages in the deep waters, that can be very costly.

After evaluating the route of a pipeline, some measures can be taken in order to mitigate probable damage in a pipeline and avoid a much bigger and irreparable problem such as a massive case of leakage in open waters. If the route chosen has a highly dynamic sea bed, or large craters that will not provide structurally safe free spans, mitigation, though expensive, will be required.

In the last years, due to the exploration of deeper seas, the need for mitigative intervention has increased. Besides that, remote and environmentally dangerous areas are being more explored these days, leaving no room for eventual in-site repairs.

Helical strakes, Fig. 20, are commonly applied for suppressing VIV of subsea tubulars. Its protuberant fins can disrupt the pattern of vortex shedding along a tubular span, which results in lower magnitudes of drag forces, and, therefore, less vibrations. In case of pipelines near the seabed, they can also help retard the sea bed scouring pattern.

Figure 20 - Helical Strakes by Lankhorst Offshore [19]

Rock dumping, Fig. 21, is a largely applied method to protect pipelines laid on the seabed. In this case a rock dumping vessel is rented and used to cover with rocks the pipeline all along. It is very cost-effective, though the pipeline is still susceptible to problems derivate from liquefaction processes, as seen in Fig. 13.

Figure 21 - Rock Dumping – Offshore fleet [20]

3. Numerical Model

This study was based on literature review and numerical analysis concerning the effect of static wave loads on free spanning pipelines. The literature review was used to find the boundary conditions of the model, as well as the right parameters to input in the analysis, in order to build a model sufficiently accurate to estimate the structural response in the pipeline and the focus of the study. Information from the literature review, such as the recommended practices and soil mechanics approach, were also used to build the model geometry and to provide its input data.

The model, which simulates an exposed pipeline enduring a wave attack while on a free spanning configuration was build using a Finite Element Method (FEM) software. With the results provided by it, a parametric analysis was conducted to analyze the sensitivity of each parameter regarding the fatigue life cumulative damage, by comparing the results of different parameters in different loads, for example. Finally, this work applied the Palm-Gren Miner rule to evaluate the cumulative fatigue damage in the pipe, considering different states occurring during the pipeline operation life.

The numerical model reproduces a static analysis configuration, with the applied loading comprising a constant hydrostatic pressure, equivalent to water depth and one cycle wave amplitude, given by a time dependent analytical field along the pipe length.

3.1 Model Implementation

The model was build using the software ABAQUS 6.14, and all the steps to its construction are explained in the following, including the definition of the boundary conditions, loading, geometry and free span parameters.

This model approaches the problem of free spanning pipelines based on a more refined method to evaluate the structural response of the pipeline in contact with the soil. It takes in consideration the soil as a solid with continuum elements. This kind of analysis is not widely used for single span analysis, as in case of 2D models, that are simpler and currently adopted [17].

Then, the innovation of the present method lies on the suitability to analyze simple configurations with a more robust approach – aiming, this way, to find how the parameters often disregarded may affect the outcome of the pipeline in general.

3.1.1 Boundary Conditions

Boundary conditions are extremely important, without them rightly put, the model often will not even run. The boundary conditions here where chosen in order to reproduce a long pipe with a single span between span shoulders, representing its continuity and support conditions.

The lower portion of the seabed, the one that is connected to the ground is set as pinned (U1 = U2 = U3). In addition, the laterals of the seabed are allowed to move only in the y-axis, so to allow the soil to behave in response to the pressure from the pipe or mean water level, as show in Fig. 22 (left).

In the Abaqus Manual [22], U1, U2 and U3 are defined, respectively, as the displacements along the x-axis, y-axis, and z-axis. While UR1, UR2 and UR3 are, respectively, the rotations around the x-axis, y-axis and z-axis.

The pipe ends are coupled to Reference Points, whose boundary conditions are guaranteeing the continuity of the pipe, as indicated on the right of Figure 22.

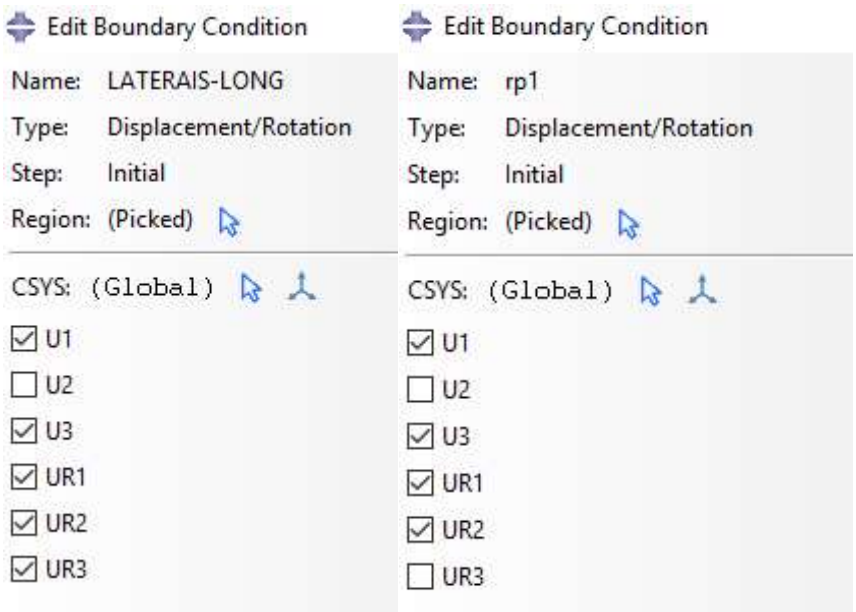

Figure 22 - Lateral of the Seabed Boundary Condition (left) and RP Fixed Pipe End (right).

It is important to mention that the gravity field in the pipe was ignored and that an initial condition of non-slip was assumed between the pipe and the soil. The pipe was assumed empty and the influence of thermal gradient was also disregarded.

3.1.2 Geometry

The geometry was based on a previous work [21], as well as DNV recommended practices and, more importantly, the need to fit and more realistic seabed into the analysis.

3.1.2.1 Span Length

The dimensions of the seabed solid were defined in relation to the pipe diameter and the span length. The main interest of this study is the upper section of the soil, where the contact happens, because of that, the depth of the soil section of the shoulders was maintained unchanged among all the analysis. While the width of the section was roughly 20 times the pipe diameter [21].

The length of the spans present in Table 3 were defined based on Table 1, and the boundary conditions used on each edge of the span assume that the pipe structure can respond with the adequate continuity.

Table 3 - Span Lengths Defined

Span Name	Span Length (m)
L1	6.5
L1	7.5
L3	8.5
L4	10

In addition, the span geometry was modeled with a realistic topography, instead of the usual idealized flat shoulders, so in case of bending, the pipe would respond to the contact of the soil immediate bellow it, as pointed in Fig. 23. Assemblies of different span length can be checked in Figs. 23-26.

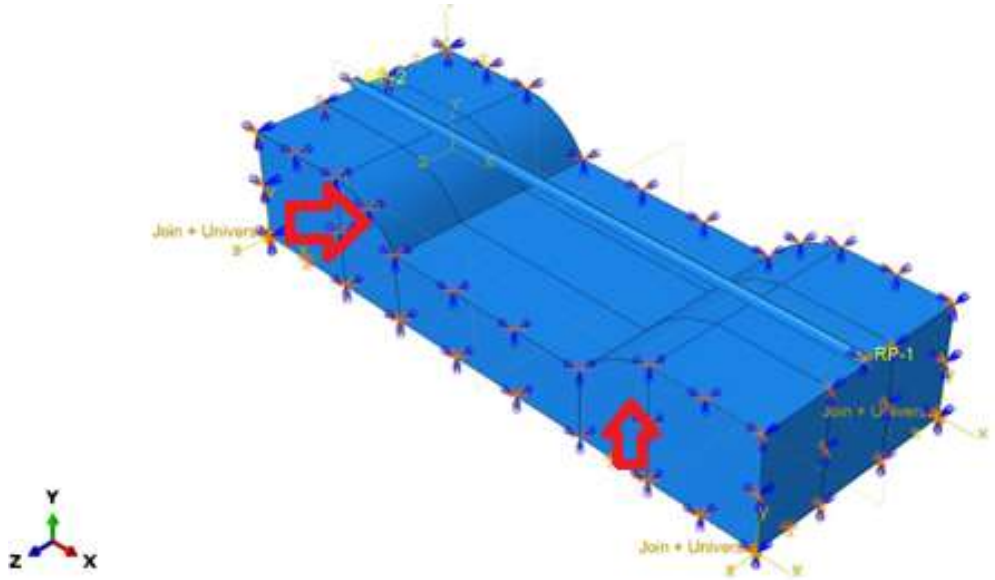

Figure 23 – Model Assembly with L=6.5m.

.

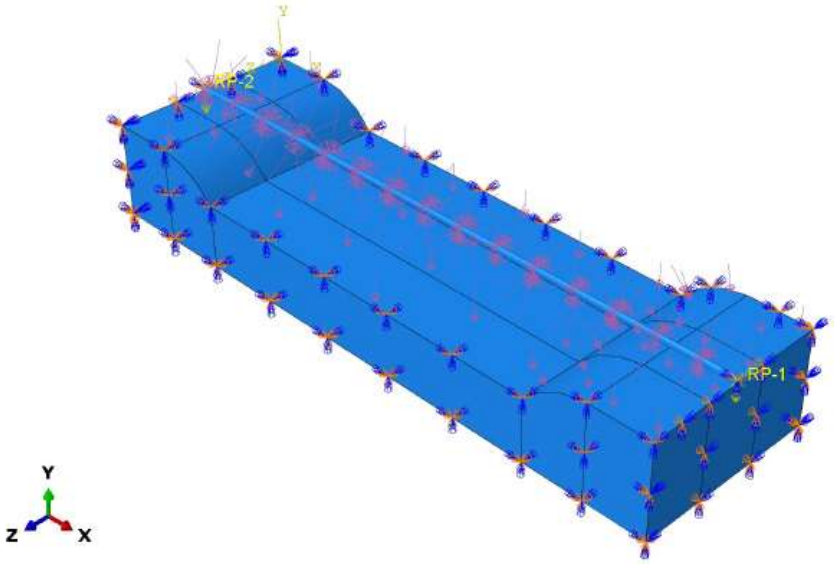

Figure 24 – Model Assembly with L2=7.5m

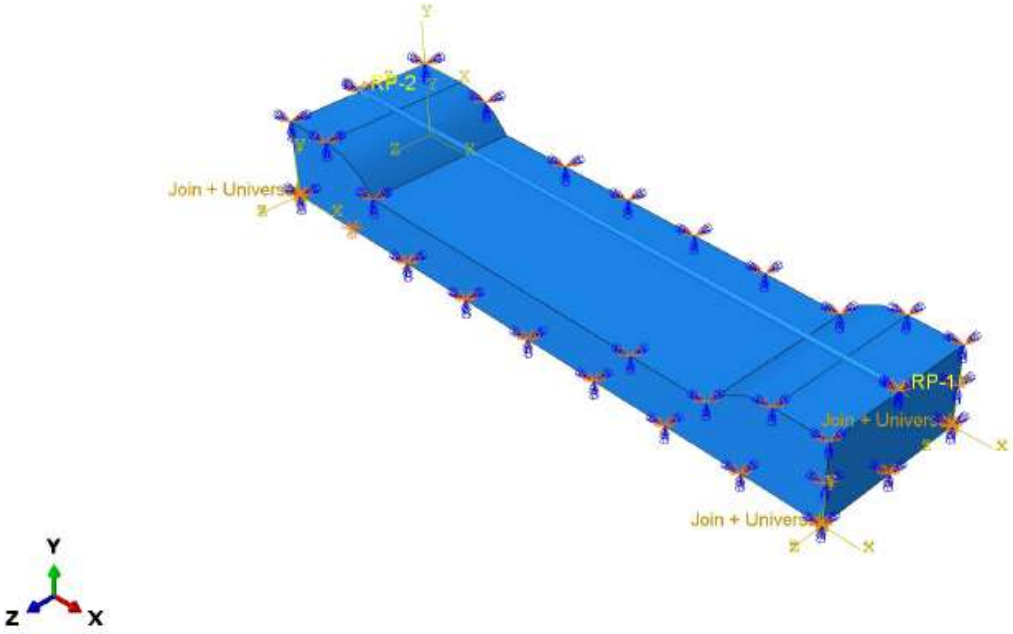

Figure 25 – Model Assembly with L3=8.5m

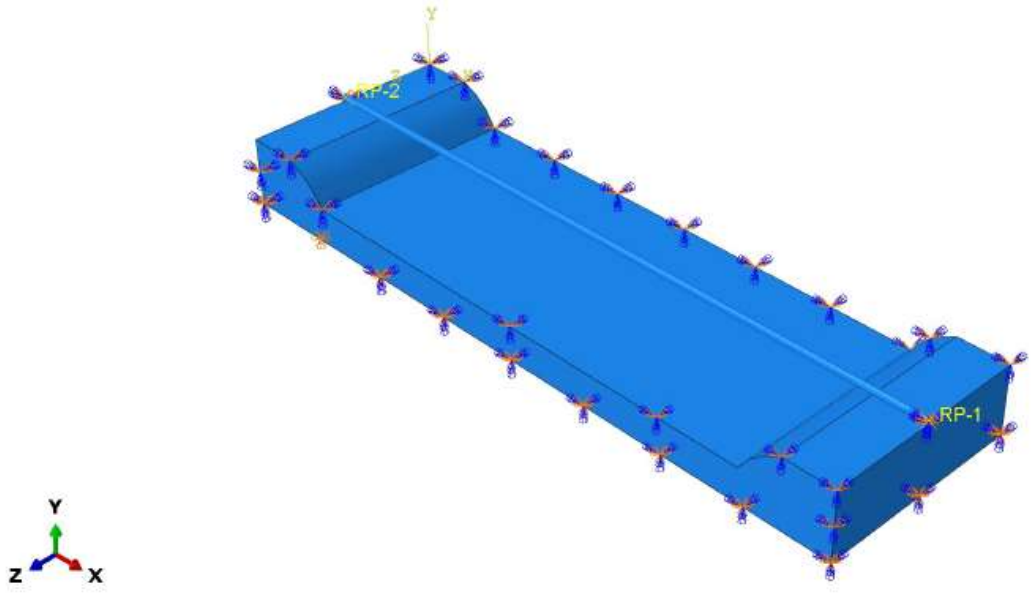

Figure 26 – Model Assembly with L4=10m

3.1.2.2 Pipe Diameter

The diameter of the pipes were chosen based on the most commercially used pipes for oil & gas industry and waste management solutions. Their values can be checked in Table 4, followed by their thickness.

Table 4 - Diameters in the Parametric Study

Diameter Name	Ø (in)	Ø(mm)	t (mm)
D1	4	101.6	10
D2	6	152.4	10
D3	8	203.2	10

In all cases of a t << Ø, the pipelines analyzed in this study can all be adequately represented by a thin-walled pipe.

3.1.3 Contact

The pipe-soil interaction is considered only on the immediate upper portion of the soil that was in contact with pipe, as well as on potential surfaces of contact, such as the seabed slope, which could interact with the pipe under bending conditions, Fig 27.

The contact was set with the surface-to-surface discretization, with the pipe being the master surface and the soil being the slave surface.

The Abaqus manual [22] defines the surface-to-surface formulation as an enforcement contact conditions in an average sense over regions nearby slave nodes rather than only at individual slave nodes. The averaging regions are approximately centered on slave nodes, so each contact constraint will predominantly consider one slave node but will also consider adjacent slave nodes. Some penetration may be observed at individual nodes; however, large, undetected penetrations of master nodes into the slave surface do not occur with this discretization.

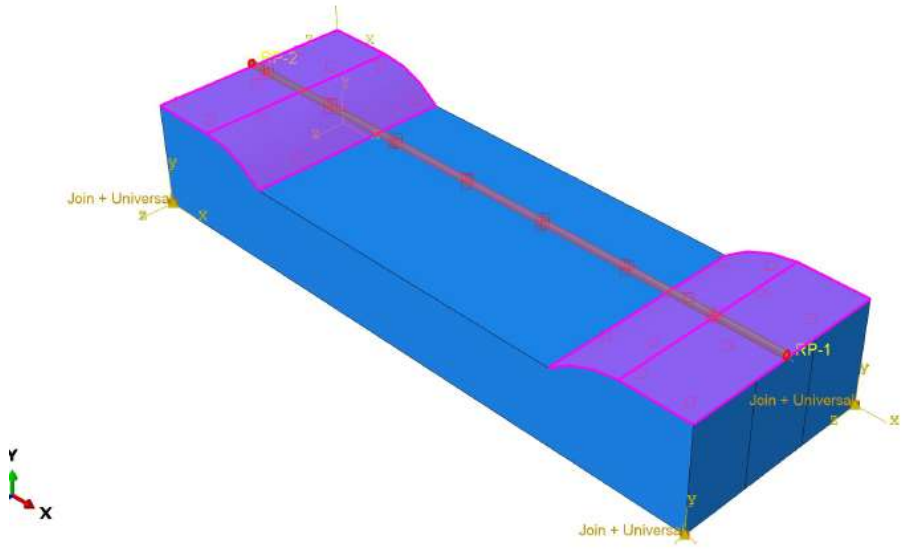

Figure 27 - Master x Slave Contact on the Model Created

The contact accounted for both tangential and normal behavior. The normal behavior has a stiffness setting that acts only when the surfaces are in compression, and there is no transfer of forces between the master surface and the slave surface when they are under tension. The normal behavior was regarded as “hard contact” and constrained with the penalty enforcement method, as seen in Figs. 28-29.

The surfaces were not allowed to separate after contact, as it would be an impossible situation when it comes about a pipeline laid on seabed under a high pressure of water weight. The “finite sliding” condition was set, since it allows any arbitrary motions over the structures.

The tangential behavior was also set with the constrained enforcement method with friction values depending on the soil used for each analysis. The directionality of the friction was assumed to be isotropic. All other contact settings for the tangential behavior were assumed the default setting.

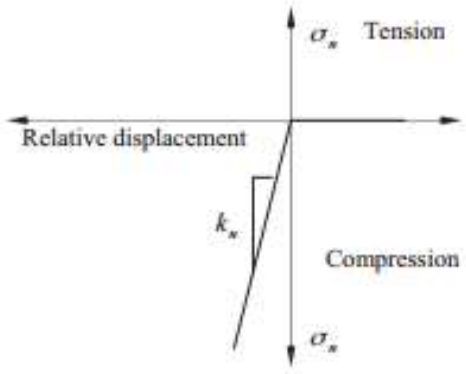

Figure 28 - Representations of Normal Contact [22]

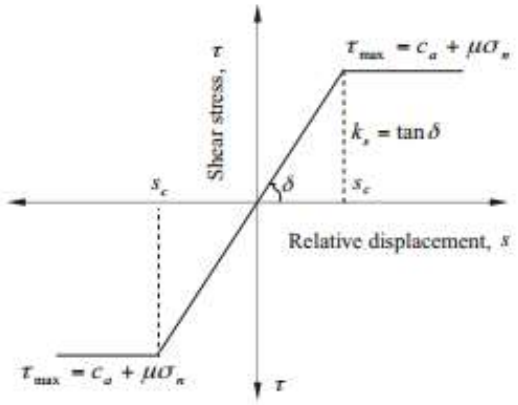

Figure 29 - Representations of Tangential Contact [22]

The friction properties in contact changed for each type of soil. The ones chosen to be used in the analysis were provided by a Naval Facilities Engineering Command (NAVFAC) standard [23], being as in the following Table 5.

Table 5 - Friction Factors in Contact

Soil Type	Steel x Soil Friction Scale
S1	0.5
S2	1

3.2 Materials

Three materials were used to implement this model, one steel and two soils. In the case of the soil, there is a limitation: since actual soil data could not be tested in the laboratory, all the soil parameters presented here are taken from the ranges available in soil mechanics literature of reliable sources.

3.2.1 Soil

The nature of soils is different from traditional materials such as steel or concrete, where the mechanical behavior can be considered linear (if the deformations do not exceed a particular limit). The mechanical properties of soils are often strongly non-linear, with irreversible plastic deformations during loading and unloading. Besides that, soils usually show anisotropic behavior, creep and dilatancy, where the latter is a volume change during shear, as stated in [26].

Because of the inhomogeneous structure of soils, their mechanical behavior is hard to predict. Assuming a linear or a section linear response can only give an approximate response and a constitutive model.

In order to implement the soil parameters into de model, some simplifications had to be made.

#1 – The soil is purely made from one material;
#2 – The material has no chance to liquefy;
#3 – The soil can be successfully described using Morh-Coulomb Theory.

3.1.2.1 Mohr-Coulomb

The Mohr–Coulomb (MC) failure criterion is a set of linear equations in principal stress space describing the conditions for which an isotropic material will fail, with any effect from the intermediate principal stress $\sigma 2$ being neglected. The Mohr-Coulomb criteria can be equalized in a function of a major $\sigma 1$ and minor $\sigma 3$ principal stress, as is detailed in Fig. 30. It can also be described as normal stress σ and shear stress τ on the failure plane [26].

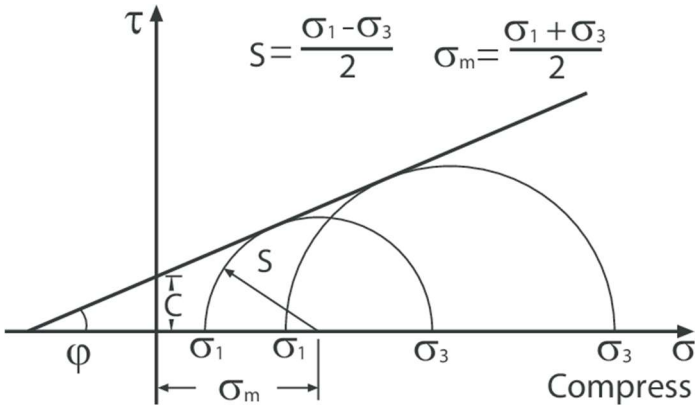

Figure 30 - Failure Envelope of the MC Criteria [26]

3.1.1.2 Soil Properties

The soil was modeled as a solid, using continuum elements. To model the soil as a solid, it is fundamental that the material is chosen right, the geometry is long/wide enough, the contact properties of the pipe and the soil are adequately assumed, and the loads are applied accurately.

The most important factor is the material prescription, especially since, as mentioned before, the mechanical properties of a soil are often strongly non-linear, even though assumed as linear, and can lead to miscalculations.

Elastic response only is usually not enough to accurately model the soil. Therefore, the importance of a pertinent plasticity model for the soil, as is the Mohr-Coulomb. The material implemented is primarily sand defined with Mohr-Coulomb plasticity, with no chance to liquefy, using parameters range defined in [27], and shown in Table 6 for S1 and S2.

Table 6 – Soil Parameters

Soil Name	Elastic Parameters		Mohr-Coulomb Parameters	
	E (MPa)	υ	ϕ	ψ
S1	50	0.3	30	0.5
S2	80	0.4	38	1

Where,

Ψ – Dilatancy angle

Φ – Friction angle

E – Young's modulus

υ - Poisson ratio

3.1.2 Steel

The composition of the steel material can very broadly. Steels, in general, have a low carbon content, and a lower amount of impurities, like phosphorus and sulfur, when compared to cast irons. In this study, a single type of steel was applied, and only its mechanical properties were addressed.

3.1.2.1 Steel Properties

The pipe material is a X-60 steel, mechanically tested in the Subsea Technology Laboratory of COPPE/UFRJ, with the results presented in Table 7 and Fig. 31 used as input in the FEA model [28]. Table 7 presents relevant mechanical properties for the API X-60 steel and Fig. 31 shows its true stress – plastic strain curve.

Table 7 – Steel Parameters

E (GPa)	υ	$\sigma_y(MPa)$	S_u(MPa)
183	0.3	520	602

Where,

E – Young modulus

υ - Poisson ratio

σ_y – Yield strength

S_u – Ultimate tensile strength

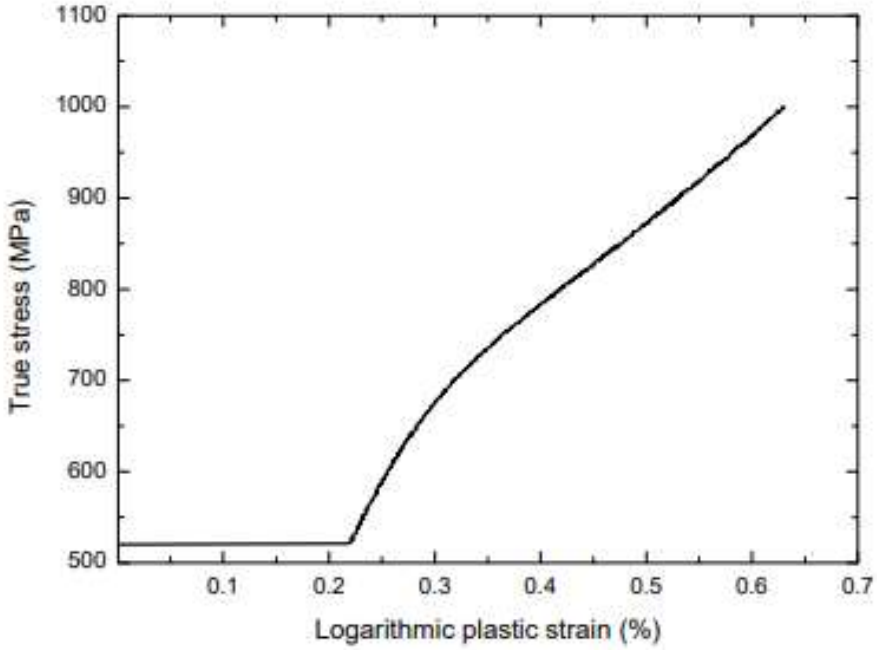

Figure 31 - True Stress x Logarithmic Plastic Strain [28]

3.2 Mesh

The elements of the mesh were chosen based on the recommended practices [17] and a previous work [27]. The soil was meshed with elements C3D8R - an 8-node linear brick, reduced integration, and hourglass control – hex dominated. The pipe was meshed with shell elements, since, as assessed before, the pipes can be considered thin-walled.

3.2.1 Mesh Sensitivity Analysis

A mesh sensitivity analysis was conducted with the aim of assuming that the results will be consistent considering different types of loads, materials and geometries in general with most efficient mesh and sufficiently accuracy, without leading to extremely high computational time for the FE analysis.

A mesh sensitivity analysis was performed for both instances of the model, analyzing the maximum von Mises equivalent in each instance. It took seven mesh refinements for the seabed instance, and six for the pipe, to get to a stabilization point, as can be seen in Figs. 32 and 33.

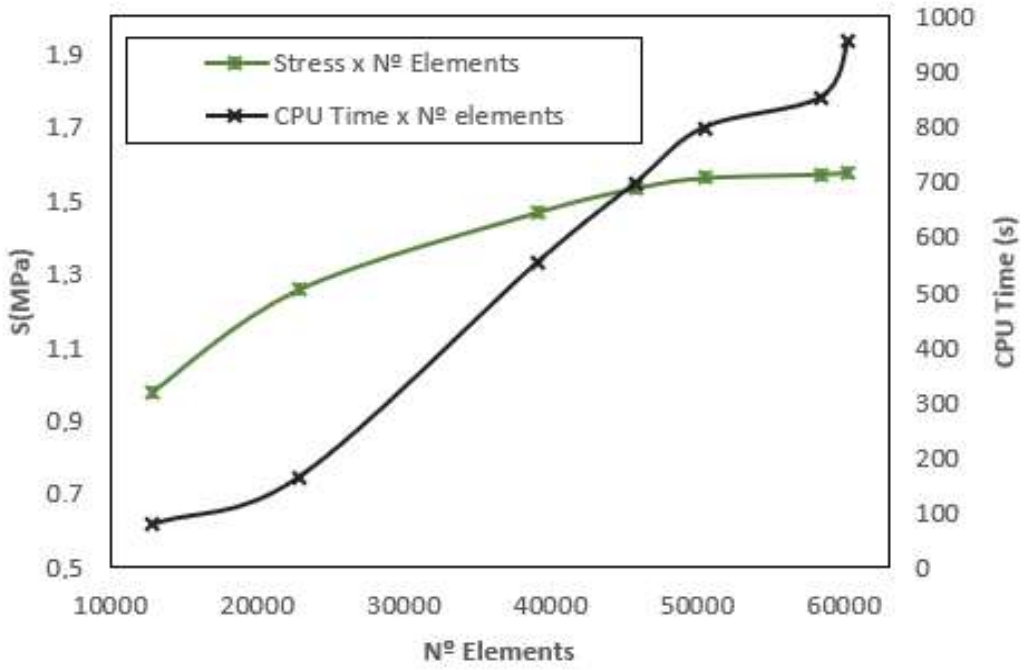

Figure 32 - Mesh Sensitivity Analysis for the Seabed Component

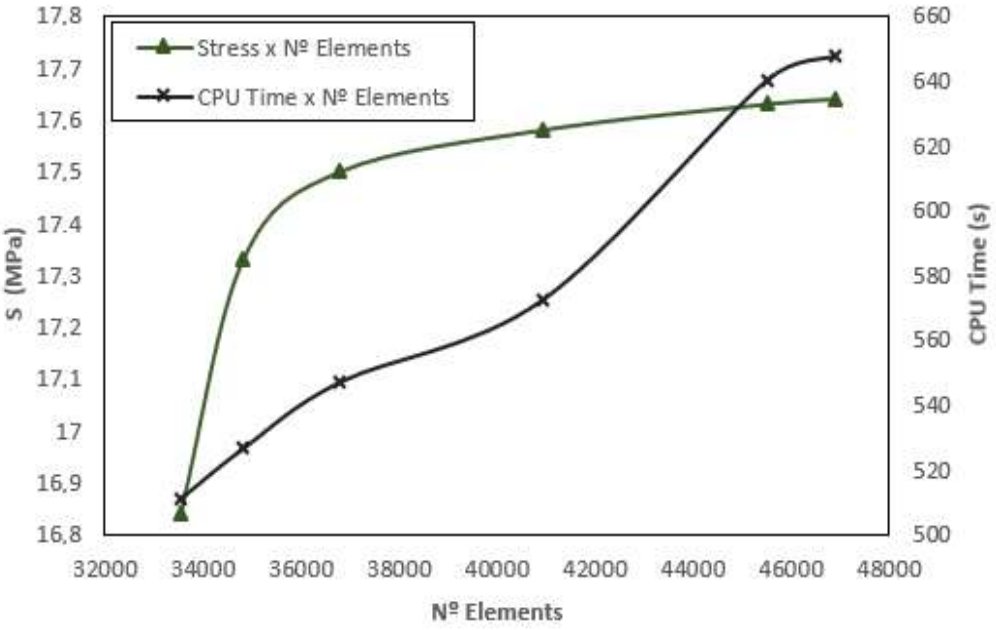

Figure 33 - Mesh Sensitivity Analysis for the Pipe Component

After a careful analysis, mesh number 5 for the seabed, and mesh number 4 for the pipe. They offered an acurate result with a reasonable computational time.

4. Wave Data Analysis

Waves represent the main and most constant form of kinetic energy transportation in the oceans. A major part of the energy that is dissipated in the shores is associated with gravity waves generated by wind and tides. The effects of surface waves are one of the concerns of coastal and marine management, since they can effectively pose a threat to the integrity of marine structures, navigation security and naval operations [24].

Wave climate study fields has two big branches: the first one is related to the seasonal variation of the waves. The second one focus on the physical wave field of the oceans and how to process its growth, propagation, and attenuation [25].

The wave climate of a region corresponds to the statistic pattern of its parameters, such as height, period, direction of propagation and dissipated energy, being closely attached to the predominant wind regime of a location, its reach, the local weather and the atmospheric system acting over it. Numerical modeling is being vastly applied in the development of wave prediction, mostly due to the lack of oceanographic data. In these days, it is popular among scientists and operational centers.

Hydrostatic and hydrodynamic loads were applied in the numerical model. Since the model was not developed as a two-dimensional problem, features such as WAVE on Abaqus could not be applied because of boundary conditions problems. The solution was to create an analytical field that would obey the wave trajectory and elevation, equation 2, using the linear wave theory [25].

$$\eta(x,t) = \text{acos}(kx - \omega t) \tag{2}$$

Also, in order to the linear theory to be valid, the waves used in this work were tested as being intermediate waters, that is:

$$\frac{1}{20} \leq \frac{h}{Lw} \leq \frac{1}{2}$$

where

h = water depth

L_w = Wave Length

This work accessed the NOAA database [6] as a source of modelled data, since it was defined as a reliable source of actual data. After analyzing the database, the data can be chosen among Field Output, Partitioned Data e Point Output. It is recommended that the partitioned data is the one chosen, as it has a built-in algorithm that quantifies the influence of the wind on the wave generation (so the waves can be classified as swell or wind sea and, in a handful of situations, can help provide the total spectrum analysis). This data is available on the FTP folder and to use it a filtering mechanism should be set to chose the data based on date, wave peaks, location, etc. The structure of the files can be checked on Annex A.

In this work, data in terms of wave height was filtered with a MatLab routine and escalated highest to lowest, in a single direction.

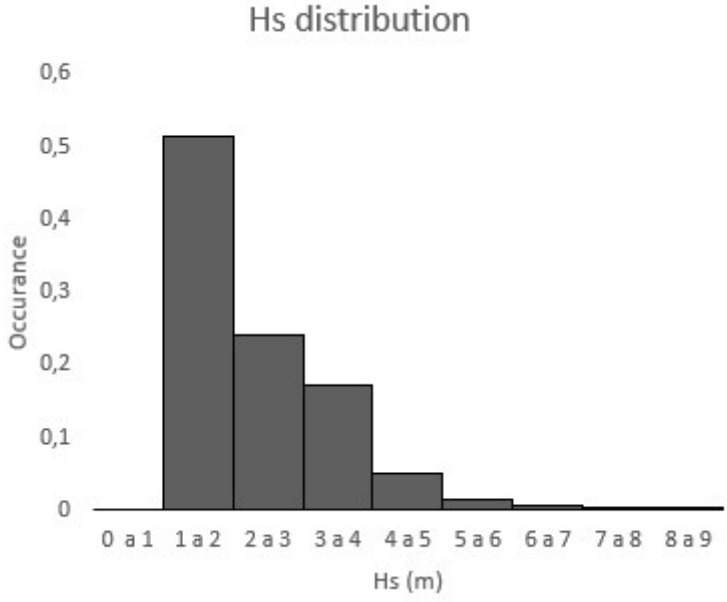

Figure 34 - Probability of Occurrence for Waves in the Glo_30 from NOAA's Database

Then, a work on estimating the design wave was developed. With this aim, all the data available should was scoured to look for the wave events that crossed substantial heights. In this work, a threshold of 5 m was established – meaning that every event beyond that level was considered to be extreme. Table 8 presents the wave heights in the x-axis and the corresponding probability of occurrence in the y-axis.

Then we proceed filling the table with values for the probability of exceedance (Q), and its negative Napierian logarithmic in order to find the curve coefficients A and B to proceed to the

calculation of the design wave, since the data is bound to conform with Weibull distribution, with

A = inclination of Hs x Q

B = intersection of Hs x Q in the vertical axis

Table 8 - Wave height Estimative for one of the Sea States

Hs band	per Hs band	sum	P	Q	lnQ
5.0 - 5.25	51	51	0.147826	0.852174	0.159965
5.25 - 5.5	111	162	0.469565	0.530435	0.634058
5.5 - 5.75	71	233	0.675362	0.324638	1.125046
5.75 - 6.0	51	284	0.823188	0.176812	1.732671
6.25 - 6.5	21	305	0.884058	0.115942	2.154665
6.5 - 6.75	14	319	0.924638	0.075362	2.585448
6.75 -7	13	332	0.962319	0.037681	3.278595
7 - 7.25	5	337	0.976812	0.023188	3.764103
7.25 -7.5	3	340	0.985507	0.014493	4.234107
7.5 -7.75	2	342	0.991304	0.008696	4.744932
7.75 -8.0	0	342	0.991304	0.008696	4.744932
8 - 8.25	2	344	0.997101	0.002899	5.843544
8.25 -8.50	0	344	0.997101	0.002899	5.843544
8.50 - 8.75	1	345 (total)	1	0	

Hs is the significant wave height, meaning that it is the average of the biggest one third wave events, with Hs band being the wave height interval.

P is the given as the fraction Sum/Total, which is the probability of non-exceedance of each band.

For this case,

$$B = 5.1$$

$$A = - 0.5074$$

Ns is the number of extreme events per years of data scoured.

$$Ns = \frac{345}{2} = 172.5 = 1/Q$$

So, rearranging and inputting the values,

$$Hss = -A*(LN(Y)-LN(Ns)) + B = 9.0 \text{ m.}$$

Where Hss is defined as the probabilistic significant wave height for a given period of time, meaning that it takes historical data to compile several significant wave heights and then, using the equations and distributions shown previously, gives a estimative of what a project wave can be.

The results for all the sea states used in the parametric study, that were defined based on the NOAA's data focusing on the most extreme cases, are shown in Table 9.

Table 9 - Sea State Definition for the Parametric Input

Sea State Name	Hs (m)	Tp (s)	h (m)
SS1	7.5	10	20
SS2	9	11	30
SS3	10	12	40
SS4	12	12	50

It is important to notice how the water depth in Table 9 increases with the wave heights. This happens because extreme waves are related with storm events, that often come accompanied with meteorological tides – which makes the level of the ocean rise for a period of time due a divergence on atmospheric pressure.

The purpose of this study is to work with extreme events, so the structural behavior of free spanning pipelines could be evaluated under critical conditions. Freaky waves present considerable danger for several reasons: they are rare, unpredictable, may appear suddenly or without warning, and can impact with tremendous force. In Fig. 34, the data shows the first ever event collected and considered to be a freaky wave. After that, several others appeared in different meteorological registers and with much more frequency, raising awareness for the change in maritime loads for offshore structures design.

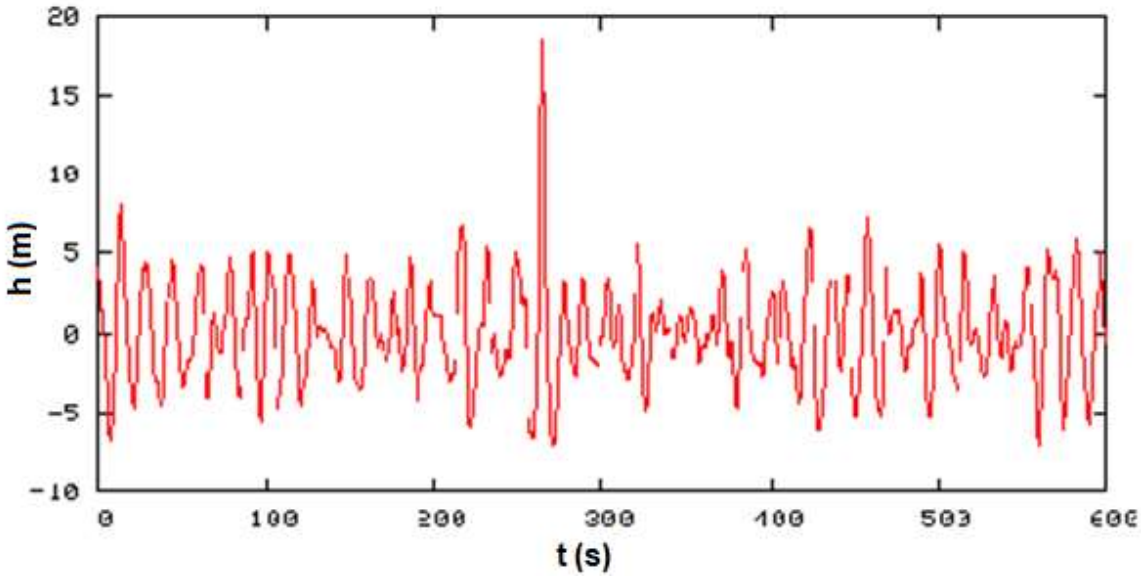

Figure 35 - First Freaky Wave Proven by Acquired Data, in Norway [24]

5. Parametric Study

Parametric studies are a largely applied method to investigate the sensitivity of a model with respect to a particular parameter. In these, a model is analyzed several times, each time varying one of its parameters.

In this work, four parameters were varied to analyze the sensitivity of the mechanical results, relatively to the maximum von Mises tension in the centroid of the pipeline: the span length, the pipe diameter, the sea state and the soil composition. These, guarded the number of changes in each parameter, totalize 96 analysis, as seen in Table 10.

The study was divided in four groups, as there were four wave heights assessed. Each of these ran with four different span lengths, two soil types and three pipe diameters, totalizing 24 analysis per group.

Table 10 - Parametric Study Cases

	Group #1	Group #2	Group #3	Group #4
Sea State	SS1	SS2	SS3	SS4
Span Length	L1 L2 L3 L4	L1 L2 L3 L4	L1 L2 L3 L4	L1 L2 L3 L4
Soil Type	S1 S2	S1 S2	S1 S2	S1 S2
Pipe Diameter	D1 D2 D3	D1 D2 D3	D1 D2 D3	D1 D2 D3
Total Combinations	24	24	24	24

4.1 Parametric Study Results

The results of the parametric study are given in four different Tables (11-14); each one of them has a fixed L, while the other parameters are varied.

All results are given in form of the von Misses stress range (Δ_σ) - that is the difference between the maximum stress to the minimum stress - in the outer part of the pipe, SNEG surface, considering the highest stress range shown in the pipe, mid-section.

Results of the output from Abaqus are presented in this section, for both the pipeline and the seabed instances.

Table 11 – Results of the Parametric Study from Analysis #1 to #24

Case	Span Length	Sea State	Diameter	Soil	Δσ (MPa)
#1	L1	SS1	D1	S1	6.98
#2	L1	SS2	D1	S1	10.12
#3	L1	SS3	D1	S1	12.39
#4	L1	SS4	D1	S1	12.87
#5	L1	SS1	D2	S1	9.28
#6	L1	SS2	D2	S1	9.77
#7	L1	SS3	D2	S1	10.13
#8	L1	SS4	D2	S1	10.38
#9	L1	SS1	D3	S1	2.57
#10	L1	SS2	D3	S1	3.56
#11	L1	SS3	D3	S1	4.43
#12	L1	SS4	D3	S1	5.88
#13	L1	SS1	D1	S2	11.85
#14	L1	SS2	D1	S2	12.35
#15	L1	SS3	D1	S2	12.70
#16	L1	SS4	D1	S2	13.19
#17	L1	SS1	D2	S2	9.41
#18	L1	SS2	D2	S2	10.14
#19	L1	SS3	D2	S2	10.40
#20	L1	SS4	D2	S2	10.93
#21	L1	SS1	D3	S2	2.57
#22	L1	SS2	D3	S2	3.55
#23	L1	SS3	D3	S2	4.43
#24	L1	SS4	D3	S2	5.98

Figure 36 presents the results dispersion from analysis #1 to #24, showing the variation between each case.

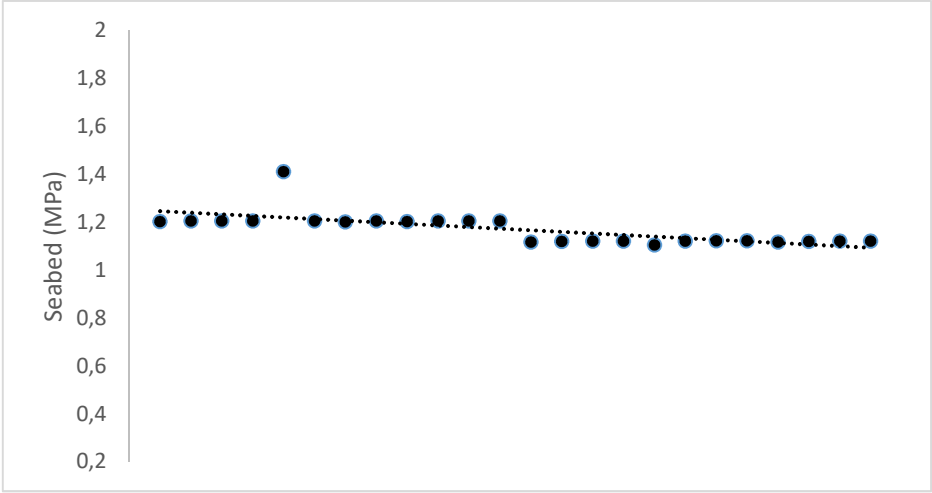

Figure 36 - Results of von Mises Stresses in the Seabed (Soil) from Cases #1 to #24

Figure 37shows the output from Abaqus for the pipeline instance, while Fig. 38 exemplifies the output from Abaqus for the seabed instance.

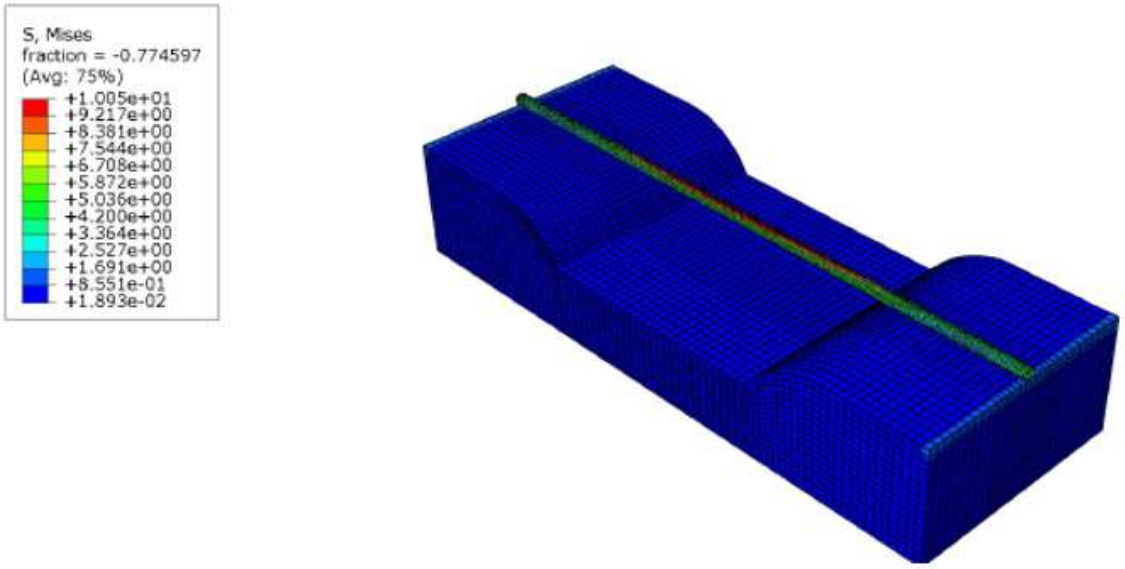

Figure 37 - Pipe Results in Terms of von Mises Stresses, SNEG (MPa) #4

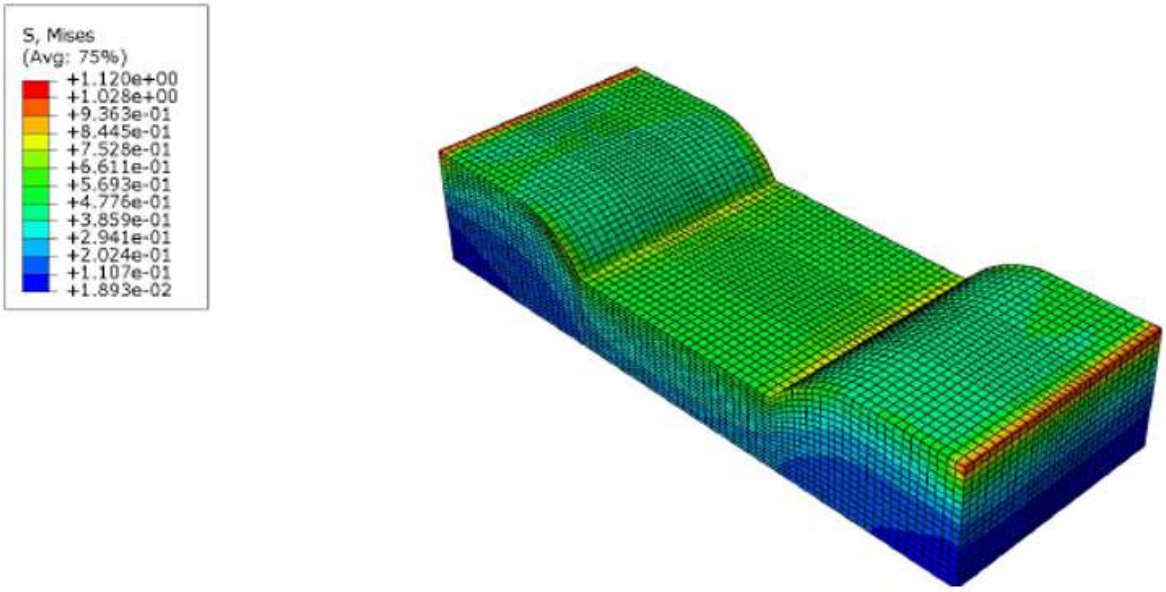

Figure 38 - Seabed Results, S, in Terms of von Mises Stresses (MPa) #4

Table 12– Results of the Parametric Study from Analysis #25 to #48

Case	Span Length	Sea State	Diameter	Soil	Δσ (MPa)
#25	L2	SS1	D1	S1	27.50
#26	L2	SS2	D1	S1	29.04
#27	L2	SS3	D1	S1	29.84
#28	L2	SS4	D1	S1	30.83
#29	L2	SS1	D2	S1	24.90
#30	L2	SS2	D2	S1	25.35
#31	L2	SS3	D2	S1	25.89
#32	L2	SS4	D2	S1	26.02
#33	L2	SS1	D3	S1	23.23
#34	L2	SS2	D3	S1	24.22
#35	L2	SS3	D3	S1	24.67
#36	L2	SS4	D3	S1	25.13
#37	L2	SS1	D1	S2	26.11
#38	L2	SS2	D1	S2	27.63
#39	L2	SS3	D1	S2	28.41
#40	L2	SS4	D1	S2	29.41
#41	L2	SS1	D2	S2	23.33
#42	L2	SS2	D2	S2	24.22
#43	L2	SS3	D2	S2	24.67
#44	L2	SS4	D2	S2	25.13
#45	L2	SS1	D3	S2	23.12
#46	L2	SS2	D3	S2	23.75
#47	L2	SS3	D3	S2	24.90
#48	L2	SS4	D3	S2	25.35

Figure 39 presents the results dispersion from analysis #25 to #48, showing the variation between each case.

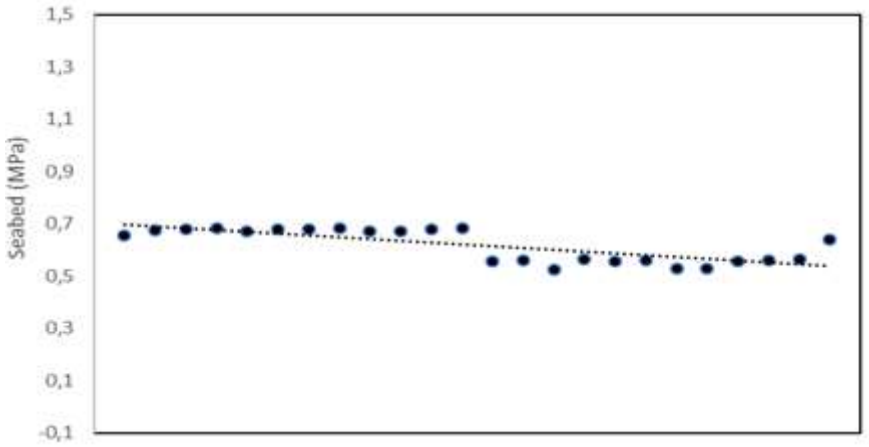

Figure 39 - Results of von Mises Stresses in the Seabed (Soil) from Cases #25 to #48

Figure 40 shows the output from Abaqus for the pipeline instance, while Fig. 41 exemplifies the output from Abaqus for the seabed instance.

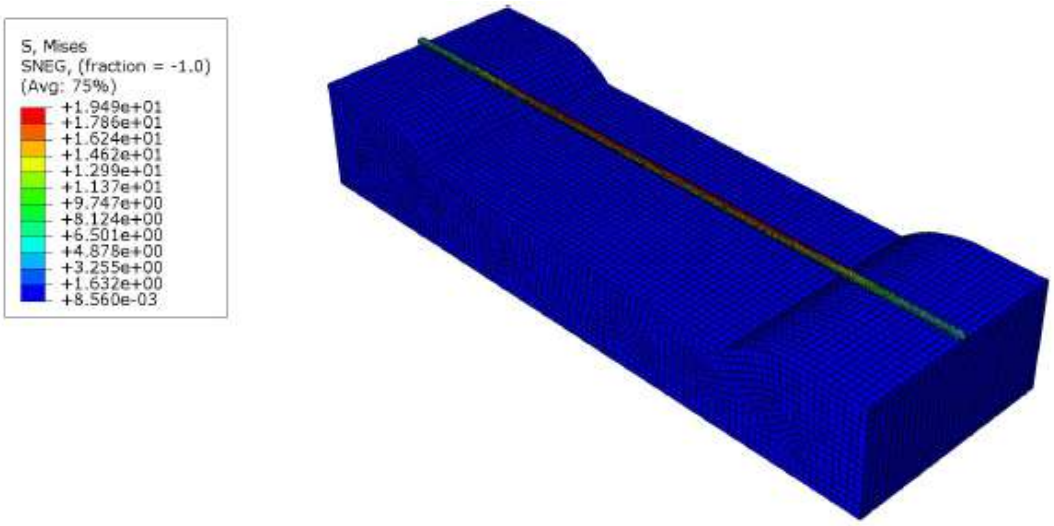

Figure 40 - Pipe Results in Terms of von Mises Stresses, SNEG (MPa) #28

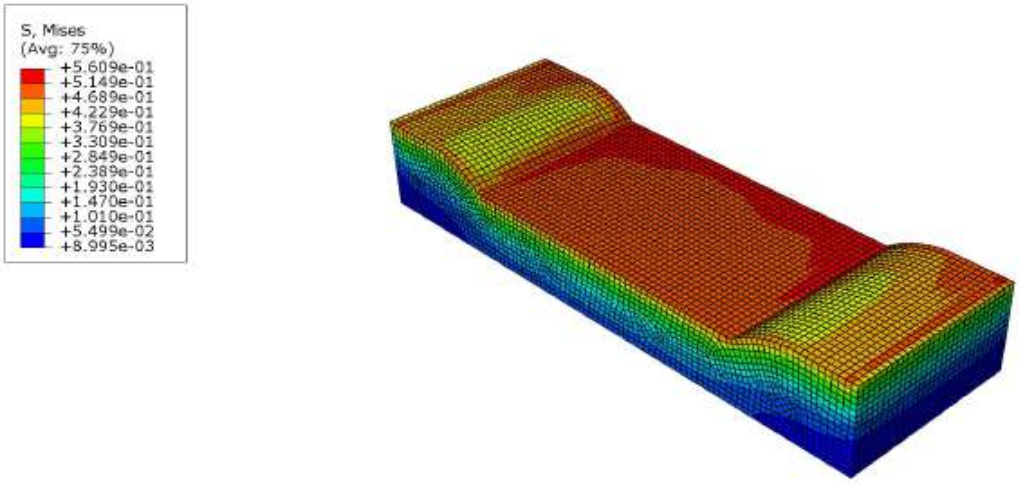

Figure 41 - Seabed Results, S, in Terms of von Mises Stresses (MPa) #28

Table 13– Results of the Parametric Study from Analysis #49 to #72

Case	Span Length	Sea State	Diameter	Soil	Δσ (MPa)
#49	L3	SS1	D1	S1	100.42
#50	L3	SS2	D1	S1	101.37
#51	L3	SS3	D1	S1	102.98
#52	L3	SS4	D1	S1	106.61
#53	L3	SS1	D2	S1	99.50
#54	L3	SS2	D2	S1	102.61
#55	L3	SS3	D2	S1	104.15
#56	L3	SS4	D2	S1	105.34
#57	L3	SS1	D3	S1	99.01
#58	L3	SS2	D3	S1	99.75
#59	L3	SS3	D3	S1	99.76
#60	L3	SS4	D3	S1	100.21
#61	L3	SS1	D1	S2	93
#62	L3	SS2	D1	S2	93.38
#63	L3	SS3	D1	S2	97.11
#64	L3	SS4	D1	S2	106.13
#65	L3	SS1	D2	S2	98.25
#66	L3	SS2	D2	S2	100.79
#67	L3	SS3	D2	S2	102.34
#68	L3	SS4	D2	S2	103.42
#69	L3	SS1	D3	S2	94.54
#70	L3	SS2	D3	S2	97.55
#71	L3	SS3	D3	S2	99.01
#72	L3	SS4	D3	S2	100.04

Figure 42 presents the results dispersion from analysis #49 to #72, showing the variation between each case.

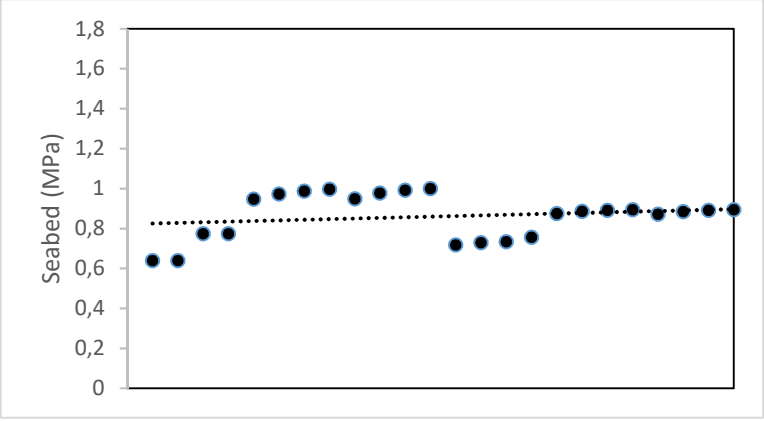

Figure 42 - Results of von Mises Stresses in the Seabed (Soil) from Cases #49 to #72

Figure 43 shows the output from Abaqus for the pipeline instance, while Fig. 44 exemplifies the output from Abaqus for the seabed instance.

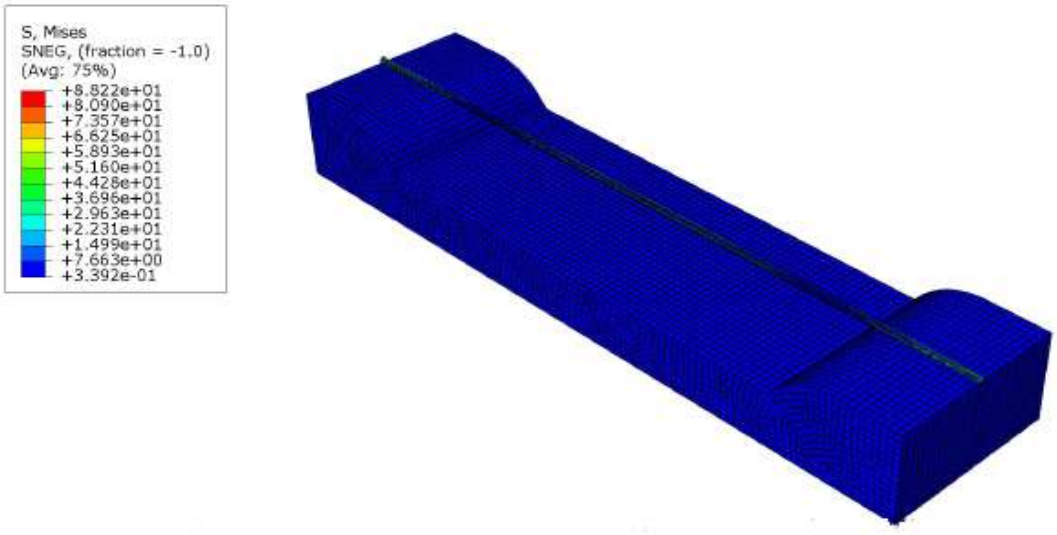

Figure 43 - Pipe Results in Terms of von Mises Stresses, SNEG (MPa) #52

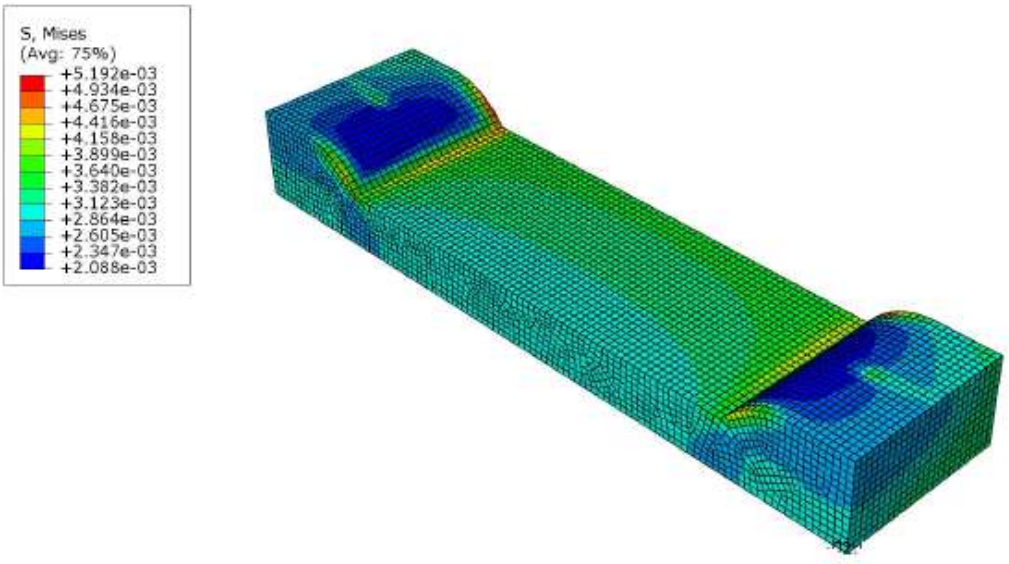

Figure 44 - Seabed Results, S, in Terms of von Mises Stresses (MPa) #52

Table 14– Results of the Parametric Study from Analysis #73 to #96

Case	Span Length	Sea State	Diameter	Soil	Δσ (MPa)
#73	L4	SS1	D1	S1	125.97
#74	L4	SS2	D1	S1	133.14
#75	L4	SS3	D1	S1	136.82
#76	L4	SS4	D1	S1	144.72
#77	L4	SS1	D2	S1	122.87
#78	L4	SS2	D2	S1	129.68
#79	L4	SS3	D2	S1	135.21
#80	L4	SS4	D2	S1	141.88
#81	L4	SS1	D3	S1	102.28
#82	L4	SS2	D3	S1	108.77
#83	L4	SS3	D3	S1	112.35
#84	L4	SS4	D3	S1	118.69
#85	L4	SS1	D1	S2	124.0
#86	L4	SS2	D1	S2	132.21
#87	L4	SS3	D1	S2	135.76
#88	L4	SS4	D1	S2	143.00
#89	L4	SS1	D2	S2	117.36
#90	L4	SS2	D2	S2	118.42
#91	L4	SS3	D2	S2	118.72
#92	L4	SS4	D2	S2	120
#93	L4	SS1	D3	S2	100.54
#94	L4	SS2	D3	S2	104.32
#95	L4	SS3	D3	S2	107.61
#96	L4	SS4	D3	S2	111.98

Figure 45 presents the results dispersion from analysis #73 to #96, showing the variation between each case.

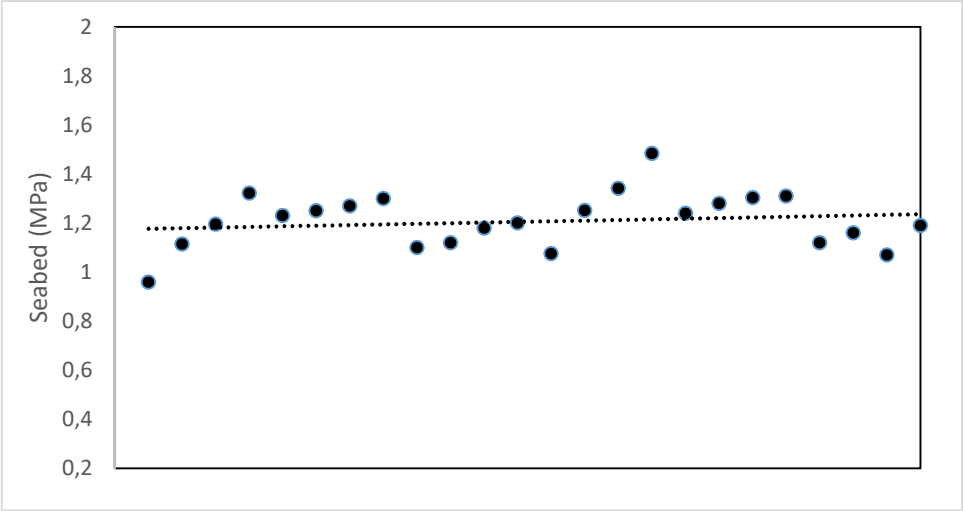

Figure 45 - Results of von Mises Stresses in the Seabed (Soil) from Cases #73 to #96

Figure 46 shows the output from Abaqus for the pipeline instance, while Fig. 47 exemplifies the output from Abaqus for the seabed instance.

Figure 46 - Pipe Results in Terms of von Mises Stresses, SNEG (MPa) #85

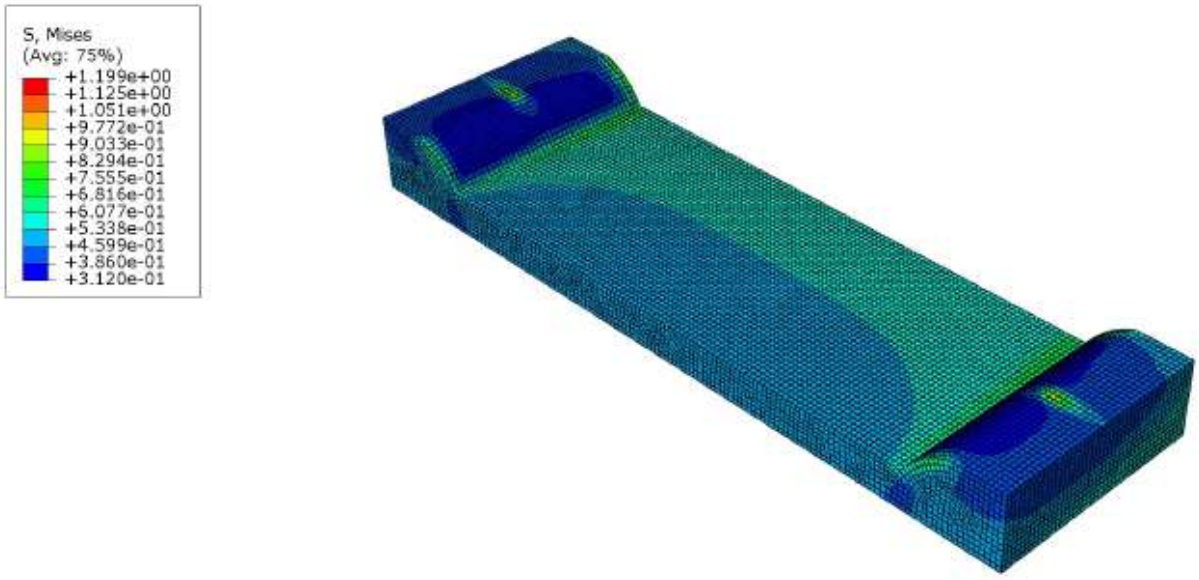

Figure 47 - Seabed Results, S, in Terms of von Mises Stresses (MPa) #85

5.2 Parameter Sensitivity and Brief Review of the FEM results

The extensive data produced from parametric studies can help to evaluate how much the change of each parameter affects the result, e.g., it is possible to evaluate how much the increase or decrease of the span length or diameter may result in an increase or decrease of the stress concentration.

This section presents a brief sensitivity analysis based on the results obtained by the parametric study (Tables 11-14) on the prior section.

All the calculations in this section are performed using the highest range of the von Mises stress output, as stated in the last section.

5.2.1 Sensitivity Regarding the Soil Type

This sensitivity analysis was performed using the most critical case of sea state, SS4, for all the span length and diameter pairs. The sensitivity was measured in percentage and took the results of soil S1 values as references, as seen in eq. 3.

$$\text{Sensitivity} = \left(\frac{S2\ results - S1\ results}{S1\ results}\right)*100 \quad (3)$$

Table 15 - Pipe Sensitivity Regarding the Soil Type

Case	Results with S1 (MPa)	Results with S2 (MPa)	Difference between Results with S1 and S2 soils (%)
L1, D1, SS4	12.87	13.19	2.5
L1, D2, SS4	10.38	10.93	5.3
L1, D3, SS4	5.88	5.98	~0
L2, D1, SS4	30.83	29.41	-4.3
L2, D2, SS4	26.02	25.13	-3.4
L2, D3, SS4	25.13	25.35	0.1
L3, D1, SS4	106.61	106.13	-0.1
L3, D2, SS4	105.34	103.42	-1.8
L3, D3, SS4	100.21	100.04	-0.1
L4, D1, SS4	144.72	143.00	-1.1
L4, D2, SS4	141.88	120.00	15
L4, D3, SS4	118.69	111.98	2.7

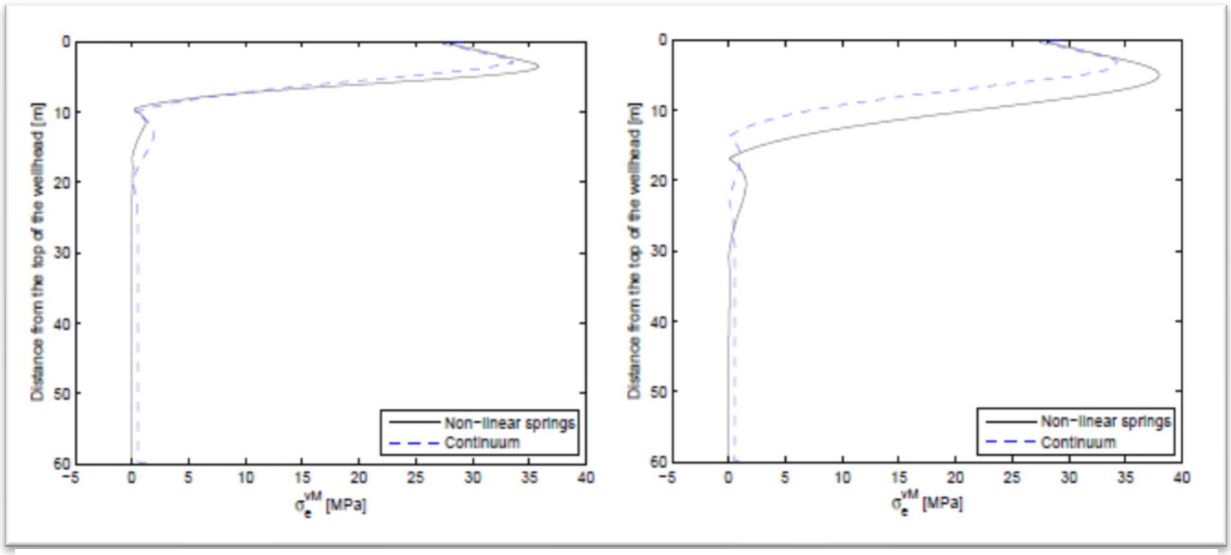

Figure 48 - Wellhead Response for a clay with E = 60 MPa (left) & Wellhead Response for a clay with E = 25 MPa (right) [21]

There was a difference in every result when regarding the change in the soil type, though it was small. This was a first investigation on how the soil can affect the response of the structure. Although it lacked some linearity, which can be explained by the non-isotropic behavior of the soil, it is clear that a change in the properties of the soil (see Table 6) can affect the results in an equal proportion. The soil properties used in this work do not differ significantly, that is because, in order to avoid computational problems and inconsistencies at first, two similar sets of soil were adopted for the analysis – both sands in the medium to hard (compacted) range, that can be described using the Mohr-Coulomb plasticity models.

In one of the works assessed by this study [21], where the soil was modeled with continuum elements in order to test the wellhead response under pressure, the author tested different kinds of soil (also comparing also with non-linear springs results), and also found that a considerable difference in the Young modulus of the soil does not lead to a significant difference in the structural response. In Fig. 48, it is noticeable that on the continuum analysis curve, the results for those two soils show similar trends.

This is usual, since due to the time-consuming methods for evaluating soils and the difficulty to accurately describe them numerically, authors tend to stick to one kind of soil (either soil, sand or silt). One good improvement would be to test all the analysis with different kinds of soil and investigate the structural response.

5.2.2 Sensitivity Regarding the Diameter and the Diameter to Thickness Ratio

Since the results seen in Table 15 showed a small sensitivity to soil types, the sensitivity towards the diameter is performed considering only one type of soil, S1, and as done before, only considering the most critical case for the sea state, SS4. Here, the lower results were taken as reference, that is the results corresponding to a larger diameter, D3, and compared with the results for the smallest diameter, D1, in all the span lengths assessed.

Table 16 - Pipe Sensitivity Regarding the Diameter 8 in to 4 in Difference

Case	Results w/ D1 (MPa)	Results w/ D2 (MPa)	Results w/ D3 (MPa)	Comparison between D1 and D2 (%)	Comparison between D2 and D3 (%)
L1, S1, SS4	12.87	10.38	5.88	24	76
L2, S1, SS4	30.83	26.02	25.13	18	4
L3, S1, SS4	106.61	105.34	100.21	1	5
L4, S1, SS4	144.72	141.88	118.69	2	18

Since the thickness was kept unchanged during the analysis, the results did not show the expected linearity for their cases. When the diameter to thickness ratio is considered, it should be noted that the adopted configurations have different D/t ratios, Table 17.

Table 17 - D/t Ratio

Diameter	D/t ratio
D1	20
D2	15
D3	10

Checking again Table 15, it is possible to note that for a fixed D/t ratio, the results respond to a certain linearity, e.g., an increase in the span length always led to a significant increase in the final pipe response.

5.2.3 Sensitivity Regarding the Sea State

This analysis is performed only for soil type S1, due to the low sensitivity of the soil type, as explained before in 4.2.1. It took in consideration the value increase from SS1 to SS4, and it is showed on Table 18.

Table 18 - Pipe Sensitivity Regarding the Sea State

Case	Sensitivity (%)
L1, D1	84
L1, D2	12
L1, D3	130
L2, D1	11
L2, D2	5
L2, D3	9
L3, D1	6
L3, D2	6
L3, D3	1
L4, D1	15
L4, D2	11
L4, D3	15

5.2.4 Sensitivity Regarding the Span Length

This analysis was fixed on soil type S1 and the most critical sea state, SS4. The results are presented in terms of change ratio instead of percentage for the sake of a better understanding. The smallest span, L1, was taken as the referential, and the largest span length, L4 was considered the final measurement, resulting in the data presented in Table 19.

Table 19 - Pipe sensitivity regarding the span length

Case	Sensitivity (x)
D1	11
D2	14
D3	19

5.3 Parametric Study Summary

After a careful examination of the results presented in Tables 11-14 and 15-19, a few points can be highlighted:

1. In all cases, a change in the soil has affected the result in terms of maximum von Mises stress amplitude in the pipeline, though the change was very small. On that matter, it is important to remember that the soils used in the analysis of the parametric results are very similar, due to computational limitations;

2. In all cases, an increase in the wave height and water depth resulted in a higher stress amplitude over the pipe;

3. A smaller diameter, as expected, is the most problematic case. The highest stress amplitudes in each table was endured by the analysis comprising a pipeline with diameter D1 (4in);

4. The difference in the structure regarding the variation of the diameter can get up to almost a 1.2 times increase, as seem in #4 and #12, and Table 15, cases with the same L, S, and SS, only varying D;

5. An increase of 3.5 meters in the span length can lead to over 10x increase in the stress amplitude, as can be checked in Table 17 and by the analysis #4 and #76, both with the same D, S, and SS, only varying L.

6. Fatigue Life Assessment

According to DNV-RP-C203 [29], the fatigue analysis should be based on S-N data, determined by fatigue testing of the considered stress concentrator, and the linear damage hypothesis. If the fatigue life estimations based on S-N data is short, indicating that a failure may occur during the service life, a more accurate investigation considering a larger portion of the structure, or a fracture mechanics analysis, shall be performed. Figure 49 shows an S-N curve for subsea pipelines, proposed in DNV-RP-C203 [29], and by its recommendation, the curve chosen is D.

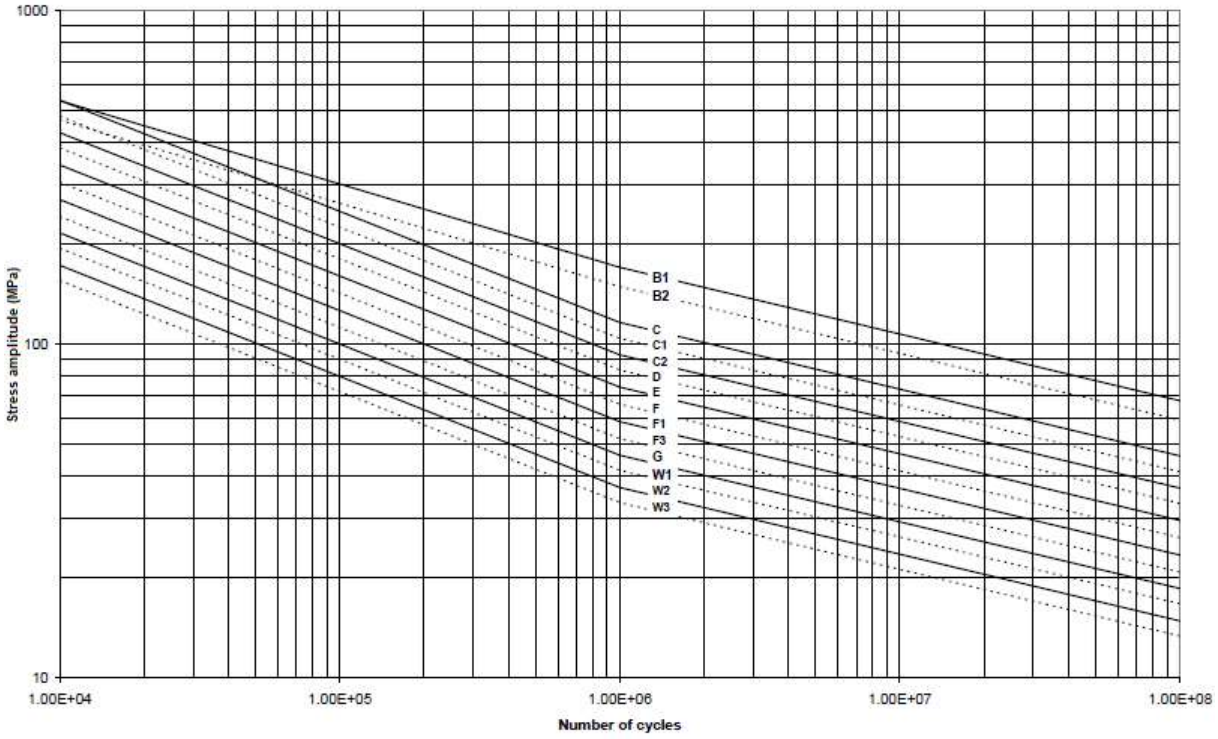

Figure 49 - S-N curves with Cathodic Protection in Seawater [29]

A fatigue analysis is usually based on an expected stress history, which can be defined as the expected number of cycles at each stress range level during the predicted life span. A practical application of this, is to establish a long-term stress range history that is on the safe side. The part of the stress range history contributing most significantly to the fatigue damage should be most carefully evaluated.

There are several ways to perform a fatigue analysis in the case of loads with varying stress ranges. One method widely used in this purpose is the Palmgren-Miner Rule, due to its simplicity and reliability.

The Palmgren-Miner rule allows the prediction of the cumulative fatigue damage when a varying amplitude loading is considered.

The Palmgren–Miner rule simply states that an individual load cycle, which is part of a variable amplitude load history, will cumulate the same fatigue damage magnitude if this load cycle is part of a constant amplitude load history [30].

Mathematically, this is expressed in equation 3.

$$D = \sum_{i=1}^{k} \frac{n}{N} \leq 1 \tag{3}$$

Where,

N = Number of cycles to failure

n = Number of cycles accumulated

D = Cumulative fatigue damage

k = Number of stress levels.

It is important to notice that when talking about steel structures in the Ocean, a design fatigue factor, DFF, must be applied to reduce the probability of fatigue failures.

According to DNV-RP-C203 and DNV-OS-C101, DFFs are dependent on the significance of the structural components with respect to structural integrity and availability for inspection and repair. This means that the more difficult it is to access a structure and repair it, a higher DFF should be considered.

DFFs shall be applied to the design fatigue life. The calculated fatigue life shall be longer than the design fatigue life times the DFF.

Table 20 - Design Fatigue Factors [30]

DFF	*Structural element*
1	Internal structure, accessible and not welded directly to the submerged part.
1	External structure, accessible for regular inspection and repair in dry and clean conditions.
2	Internal structure, accessible and welded directly to the submerged part.
2	External structure not accessible for inspection and repair in dry and clean conditions.
3	Non-accessible areas, areas not planned to be accessible for inspection and repair during operation.

With the definition given by Table 20, the analyzed case would be related to a DFF of 2, as it concerns an external structure not accessible for inspection and repair in dry and clean

conditions. The failure probability for the S-N curves is given by DNV [29], as shown in Fig.50, based on the use of design factors.

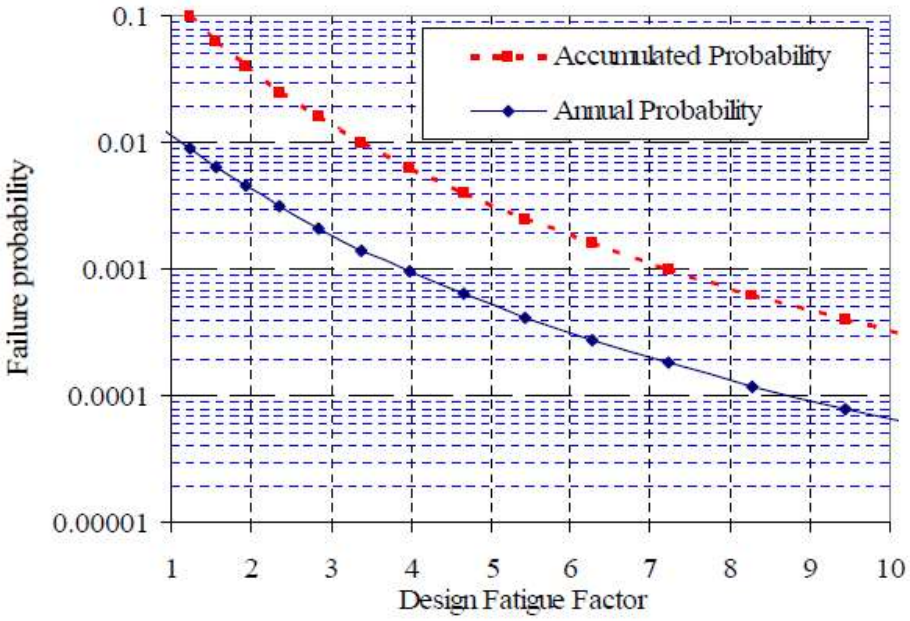

Figure 50 - Failure Probability as a Function of the Design Factor [29]

To be able to use the S-N curve presented in Fig. 49, the results of the parametric study must undergo a correction, since the cyclic loading presents a mean stress component. To perform it, the Goodman criterion is applied. The Goodman criterion [31] is used to evaluate the influence of mean and alternating stresses on the fatigue life of a material, and it can be described as showed in equation 4.

$$\frac{\sigma_a}{S_f} + \frac{\sigma_m}{S_u} = 1 \tag{4}$$

Where,

σ_a – Stress amplitude

σ_m – Mean stress

S_f – Fatigue limit for a completely reversed load

S_u – Ultimate tensile strength

With $S_u = 602\ MPa$ for the X60 steel used in this analysis. Table 21 presents the corrected stress amplitudes for a fully reversed stress cycle ($\sigma_m = 0$), that will be used in the fatigue life assessment.

Table 21 – Stress difference corrected for Sm=0

Case	S_f(MPa)	Case	S_f(MPa)	Case	S_f(MPa)	Case	S_f(MPa)
#1	3.510351	#25	14.0714	#49	54.77885	#73	70.34493
#2	5.102891	#26	14.87887	#50	55.34471	#74	74.84665
#3	6.259414	#27	15.29918	#51	56.30593	#75	77.18064
#4	6.504529	#28	15.82009	#52	58.48351	#76	82.2459
#5	4.676041	#29	12.71292	#53	54.23178	#77	68.41706
#6	4.924964	#30	12.94761	#54	56.08478	#78	72.66677
#7	5.107977	#31	13.22948	#55	57.00623	#79	76.15754
#8	5.235133	#32	13.29737	#56	57.72002	#80	80.4163
#9	1.287749	#33	11.84351	#57	53.94078	#81	55.88767
#10	1.780249	#34	12.35861	#58	54.38035	#82	59.78611
#11	2.22318	#35	12.59303	#59	54.38629	#83	61.9564
#12	3.004925	#36	12.83285	#60	54.65389	#84	65.835
#13	5.983895	#37	13.34439	#61	50.39244	#85	69.11852
#14	6.238996	#38	14.13948	#62	50.61566	#86	74.25934
#15	6.417695	#39	14.54829	#63	52.81484	#87	76.5067
#16	6.668049	#40	15.07319	#64	58.19474	#88	81.13666
#17	4.742062	#41	11.8955	#65	53.48994	#89	65.0176
#18	5.113062	#42	12.35861	#66	54.99912	#90	65.6689
#19	5.245308	#43	12.59303	#67	55.9235	#91	65.85346
#20	5.515066	#44	12.83285	#68	56.56912	#92	66.64207
#21	1.287749	#45	11.78633	#69	51.298	#93	54.85027
#22	1.780249	#46	12.11396	#70	53.07524	#94	57.1081
#23	2.22318	#47	12.71292	#71	53.94078	#95	59.08593
#24	3.004925	#48	12.94761	#72	54.55277	#96	61.73143

6.1 Fatigue Life Consumption Calculation

The fatigue life assessment was calculated using the Palmgren Miner rule [32], with the data displayed in Table 21, and the S-N curve D presented in Fig. 48.

For each combination of soil, pipe diameter and span length, the sea state is varied four times; each of the variations represents a probability of 25% of a certain wave occurrence and depth driven by tide, summing up a total of 100% occurrence.

The wave occurrences were defined according to NOAA database and calculations described in Annex A. A histogram was obtained based on the selected data, identifying pairs of significative wave and peak period for probabilities of occurrence of 25%, 50%, 75% and 100%.

The case of analysis numbered #1 to #48 stayed under the risk of fatigue damage, as their stress amplitude range stayed well below the S-N curve.

The results will be demonstrated in 12 blocks, regarding analysis #49 to #96. Each of them has the span length, diameter and soil, and a varying sea state, that will be used as increment for the Palmgren-Miner rule.

- Block #1 – Analysis #49 to #52

  $D = \sum_{i=1}^{4} \frac{n}{N} = 0.15 \leq 1$

- Block #2 – Analysis #53 to #56

  $D = \sum_{i=1}^{4} \frac{n}{N} = 0.15 \leq 1$

- Block #3 – Analysis #57 to #60

  $D = \sum_{i=1}^{4} \frac{n}{N} = 0.16 \leq 1$

- Block #4 – Analysis #61 to #64

  $D = \sum_{i=1}^{4} \frac{n}{N} = 0.34 \leq 1$

- Block #5 – Analysis #65 to #68

  $D = \sum_{i=1}^{4} \frac{n}{N} = 0.21 \leq 1$

- Block #6 – Analysis #69 to #72

$D = \sum_{i=1}^{4} \frac{n}{N} = 0.0.32 \leq 1$

- Block #7 – Analysis #73 to #76

  $D = \sum_{i=1}^{4} \frac{n}{N} = 0.04 \leq 1$

- Block #8 – Analysis #77 to #80

  $D = \sum_{i=1}^{4} \frac{n}{N} = 0.05 \leq 1$

- Block #9 – Analysis #81 to #84

  $D = \sum_{i=1}^{4} \frac{n}{N} = 0.12 \leq 1$

- Block #10 – Analysis #85 to #88

  $D = \sum_{i=1}^{4} \frac{n}{N} = 0.12 \leq 1$

- Block #11 – Analysis #89 to #92

  $D = \sum_{i=1}^{4} \frac{n}{N} = 0.20 \leq 1$

- Block #12 – Analysis #93 to #96

  $D = \sum_{i=1}^{4} \frac{n}{N} = 0.20 \leq 1$

6.2 S-N Analytical Curve Evaluation

While DNV S-N diagrams are very useful, reliable, and ready to use on design matters, though they do not allow a consistent investigation of physical response of the structure. This happens because of the numerous safety and correction factors that are implicit on these recommended practices curves, such as the temperature factor, reliability factor, surface finish factor, etc.

One in particular, the often described as "miscellaneous factor", is very difficult to quantify and, therefore, to evaluate when analyzing the material response. It can account for the influence of corrosion, electrolytic plating, metal spraying, fretting corrosion and radiation effects on materials.

Since the present study concerns the high cycle regime, the methodology adopted for defining the analytical S-N curve considers fatigue lives higher than 1000 cycles.

6.2.1 Plotting of the Analytical S-N Curve

S-N analytical curves can be built using data based on mechanical tests and a series of empirical equations. In addition, two different methodologies are usually adopted in the formulation of an S-N analytical curve, [34]. One of them comprises both low cycle fatigue and high cycle fatigue regime, which ranges from 1 to 1000 cycles. And the other one is when only high cycle fatigue is considered, ranging from 1000 cycles and up.

For this study, only the high cycle fatigue is pertinent, therefore, the S-N analytical curve presented in this section starts at 10^3 cycles.

The S-N curve can be approximated using the Basquin equation [33]:

$$S_f = CN^b \quad \text{(Eq. 4)}$$

Where

S_f is the fatigue strength and C and b are material parameters.

To estimate the value of C in for this work, the equation 5 was used.

$$C = \frac{(f * S_u)^2}{S_e} \quad \text{(Eq. 5)}$$

Where f is value depending on S_u, Table 22.

Table 22 – Variation of f with S_u [33, 34].

$S_u\ (MPa)$	f
414	0.93
621	0.86
828	0.82
1380	0.77

The fatigue limit S_e can be estimated as

- $S'_e = 0.5S_u$ if $S_u < 1400$ MPa
- $S'_e = 700$ if $S_u > 1400$ MPa

The b estimative is given as

$$b = -\frac{1}{3} log\left(\frac{f * S_u}{S_e}\right) \quad \text{(Eq. 6)}$$

So, finally, the equation describing the analytical curve for the API X-60 steel used in this work is given by Eq. 7, and its plot on Fig. 49.

$$S_f = 911N^{-0.08} \quad \text{(Eq. 7)}$$

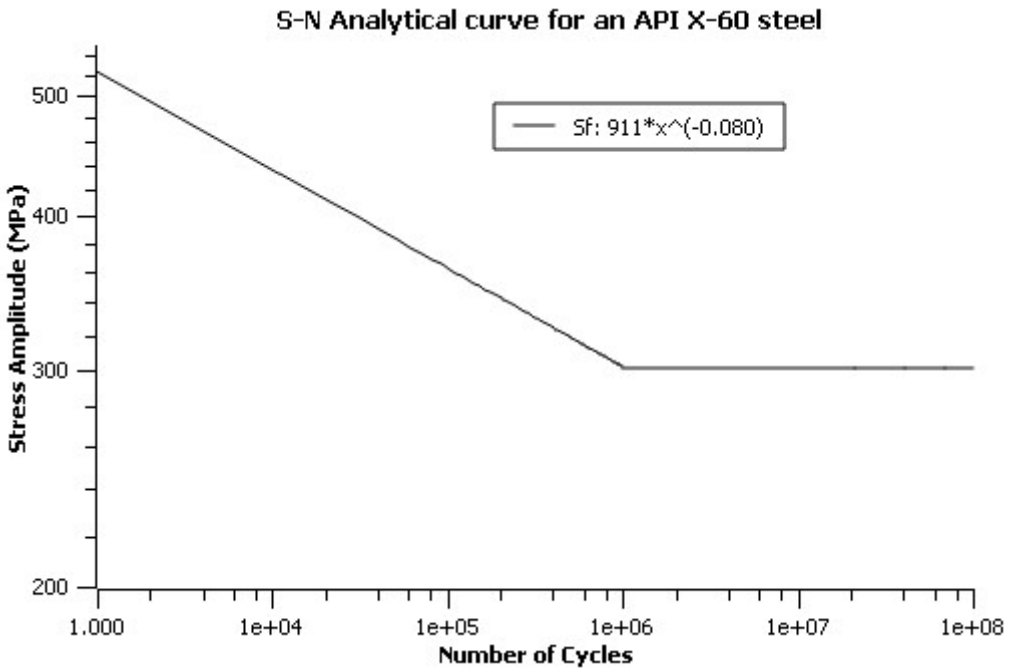

Figure 51 - S-N Analytical Curve with no Safety or Correction Factors Implicit

When using the load data from Table 21 into the analytical S-N curve develop, Fig.51, all analyzed cases lie in the infinite life domain, meaning that they do not lead to fatigue life consumption, while half of the results ended up with some level of fatigue damage accumulation when using the DNV S-N curve. This happens because of the numerous safety and correction factors implicit in the DNV curve, after all, it is not purely a structural analytical curve and yes, a design curve.

It raises the question of how conservative the design practices available today are. The actual need of mitigation could be critically evaluated if the structure response, the loading and all the interaction were more tacit. Furthermore, it is important to remember that are different methodologies to plot S-N curves and that there are different problems and challenges to incorporate into the security factors, and the right choice is often dependable of how well the project site environment is known, the material and the purpose of the structure.

In this work, only one wave passage direction and the water pressure were considered as applied loading. In a real environment, there will be waves coming from multiple directions, intermittent load of the currents, thermal gradient in the pipes, chemical incrustation, etc. happening to the structure. Therefore, the safety factors are very important, but it should be noted that it is more valid and accurate to know the installation site and research about its

environment and loads to avoid using far too conservative safety factors and increasing, unnecessarily, the cost of a project.

7. Conclusions

From the literature review, it becomes clear how many challenges the pipeline design can face when it comes about free spans. The literature review comprised a brief assessment of the recommended practices, that are often very statistic-oriented and conservative. In addition, this work meant to explain the different phenomena such as liquefaction and sediment transport, that can lead to a free span.

Pipeline design, when taking into consideration different free span configurations and its interaction with the soil, can be complicated, so hopefully the results presented in this work can helpful to other studies in order to avoid some uncertainties and to understand how big of a part an in-line wave loading can play in the cumulative fatigue damage.

As explained before when reviewing the results of the parametric study. In all cases, a variation of soil has affected the result in terms of maximum stress amplitude in the pipeline, though the change is very small. On that matter it is important to remember that the soils used in those analysis are very similar, due to computational limitations.

Only one case showed a significant difference, as can be seen in Table 14, the analysis on that was once more ran, giving the same results. One probable cause for this can be how much the pipe interacted with the soil, as it is set on the largest span length and therefore has a bigger chance of bending. That can also be the reason of some small instabilities in the seabed results as the span length is increased.

The intensification of the sea state, that is, the significant wave height, peak period and water depth, has resulted in a higher stress amplitude over the pipe in all cases, in Table 16 can be noted that the smallest span, L1, is more sensitive to this increase of wave loads, nevertheless, this can be explained by the small numbers of the stress amplitudes found with this span length case, as one of the results escalated from 6 MPa to 13.3 MPa (from SS1 to SS4). The combination between the largest span length, with smallest diameter reached over 144 MPa on the most critical sea state.

The difference in the structure regarding the variation of the diameter can get up to 115%, when comparing the biggest diameter to the smallest diameter. In the three largest span lengths – L2, L3 and L4 -, the percentage of the difference between the results considering D1 and D3 fell among the same order of magnitude. In other hand, the smallest span length showed a big

percentage difference, but again, it could be explained by the small result number that were found when analyzing the cases with that span length.

Regarding the longest free span, L4, half of the cases with this span length accused a mild cumulative fatigue damage sum. It should be noted that, since the free spans all start with small gaps and lengths, and some of them start from scratch, it is worrying to see that a difference of 3 meters in the length of the span can add up to a damage over 10x worse than in the original configuration. For that reason, even looking very conservative, the DNV's RP-F-105 is not.

This work assessed only in-line wave loads over the pipeline, that are often disregarded as they are not considered so damaging in terms of fatigue life consumption because of the lack of flow around the pipe, and therefore vibration. Even isolating the least harmful wave loads, this study indicated a cumulative fatigue damage reaching 34% for a pipeline in free spanning configuration, according to the DNV S-N curve. However, during operation subsea pipelines are expected to endure harsh environmental attacks, and a real life scenario would include, in the case of free-spanning pipelines, besides the lack of support, loads coming from intermittent currents that will generate VIV, different wave directions, thermal gradients, cyclic internal pressure, etc. and because of it, a fatigue life consumption around 30% due to only in-line wave loads may significantly contribute to fatigue damage computing considering the different sources of cyclic loads. Furthermore, it seems logical that this behavior is due to the free span configuration. For this reason, knowing the pipeline route environment and the source of cyclic loads it will be exposed to is crucial.

Another crucial matter is to know what kind of safety factors should be applied, inputing the right and specific factors for the case would protect the structure and avoid a project design that is too conservative and, therefore, expensive. As it could be noted from the fatigue assessment in this study, if the concern was only one specific type of wave, the DNV-RP-F105 would have been far too conservative, so the understanding of the structure response, and its interactions with the surrounding environment, and defining the pertinent cyclic loads concerned are crucial for a proper structure design, which could also avoid unnecessary future mitigation interventions.

The only way to obtain reduced cost of mitigation is to understand better the interaction between soil, structure and fluid. There are some formulas and software to calculate and foresee the free span possibilities and lengths, but free spanning pipelines are highly dependent on the wave climate of a region, and in the current state of the world, this is bound to be changing in more-rapid-than-ever pace. For these reasons, the interaction between structure, soil and fluids

should be studied continually in order to keep up the pace with the climate change that disturbs how the ocean loads behave and how they affect offshore structures.

8. Future Works

This work is a first step to path the way of future studies. Even with all the limitations, the results were consistent. Following is a list of improvements that must be done regarding this thesis' work.

1. Use larger range of soil types, especially different sized ones. Such as clay and pebbles, and compare the values between them, as in the literature, authors tend to stick to one kind of soil (in this work it was sand) in order to avoid time-consuming modeling for the continuous elements;
2. Use more than one kind of metal, so the pipe material can be included as in parametric sensitivity study;
3. Try to apply composites as the pipe material;
4. Change the inclination of the slope modeled. This way, inconsistent soils results can be avoided;
5. Change the thickness of the pipe in order to maintain the same diameter-to-thickness ratio and avoid inconsistences in the results, since using dimensionless analysis can lead to better comparisons regarding the parametric study;
6. Implement dynamic analysis in order to study the impact of the VIV phenomena alone and combined with waves;
7. Test the soils in a lab instead of taking them from the literature;
8. Compare different recommended practices available. In this work, Only DNV's was used here;
9. Analyze this work with beam elements, so a more accurate analysis of the pipe-soil interaction can be performed – The Abaqus library provides specific elements (PSI34 and PSI36) for the 3-D pipe-soil interaction process, being very useful to analyze the interaction between a semi-buried pipeline and the surrounding soil.

Besides that, it is always important to remember that free spanning pipelines are a very multidisciplinary subject and should be discussed with different specialists.

9. References

[1] UNISDIR (United Nations Office for Disaster Risk Reduction). https://www.unisdr.org/we/inform/disaster-statistics Accessed in 08/10/18

[2] MUNICH RE. Scientific facts and economic impacts of natural disasters. 56 pg. Retrieved from www.munichre.com Accessed in 02/10/18

[3] EUROSTAT. Energy Statistics. https://ec.europa.eu/eurostat/statistics-explained/index.php/Energy Accessed in 05/10/18

[4] PULSE MONITORING STRUCTURAL MONITORING. https://www.pulse-monitoring.com/ Accessed in 16/11/18

[5] Scour and Scour Protection, US Army Training Course. Lecturer Steven Hughes, phd. Retrieved from http://www.oas.org/cdcm_train/courses/course4/chap_8.pdf. Accessed 20/04/2018

[6] NOAA Database ftp://polar.ncep.noaa.gov/pub/history/waves Accesed 07/07/2018

[7] MAZZINE, A. et al. (2017) A climatic trigger for the giant Troll pockmark field in the northern North Sea. Earth and Planetary Science Letters, Vol 464 – P. 24-34

[8] Natural Resources Defense Council "Permafrost and Everything you need to know" https://www.nrdc.org/stories/permafrost-everything-you-need-know Access in 28/10/18

[9] PEW Research. "Artic Standarts – Full Report" Retrieved from https://www.pewtrusts.org/en/ Access in 21/04/2018.

[10] HUGHES, S.A; KAMPHUIS, W. Scour at Coastal Inlet Sctructures. Proceedings of 25th Conference on Coastal Engineering. Capítulo 175, pág. 2258-2271. Orlando, Florida, 1996.

[11] DAY & SUBACH. 2014. "Fluvial Hydrodynamics" 362p. Springler. Spain.

[12] WHITEHOUSE AND HARRIS. Scour Prediction Offshore and Soil Erosion Testing. Proceedings of OMAE 2014. San Diego, California, USA.

[13] SUMER, B.M.(2014) Liquefaction Around Marine Structures. World Scientific, 2014. 439p. Coleção Advanced Series on Ocean Engineering. Volume 39.

[14] VAN RIJIN, L.C., 1993, 2012. Principles of sediment transport in rivers, estuaries and coastal seas. Aqua Publications, Amsterdam, The Netherlands.

[15] WATERKEMPER, J., 2015 “Estudo Experimental sobre a erosão Induzida por Ondas ao Redor de Dutos submarinos” Federal University of Rio Grande (Bachelor’s degree final thesis). Retrieved from ARGO – FURG.

[16] SUMER, B.M.(2014) Liquefaction Around Marine Structures. World Scientific, 2014. 439p. Coleção Advanced Series on Ocean Engineering. Volume 39.

[17] DNVGL-RP-F105 – Free Spanning Pipelines. Published by DNVGL on April 1, 2017

[18] DNVGL-RP-F114 – Pipe-soil interaction. Published by DNVGL on April 1, 2017.

[19] Lankhorst Offhore institutional website, https://www.lankhorst-offshore.com/en/viv-strakes, acesssed on 15/02/2019.

[20] Offshore Fleet Institutional website http://offshore-fleet.com/data/rock-dumping-vessel.htm, accessed on 15/02/2019.

[21] STROMBLAD, N., 2014 “Modelling of Soil and Structure Interaction Subsea”. Chalmers University (Master’s Degree Thesis). Sweden. Retrieved from Chalmers Publication’s Library.

[22] Abaqus User Manual. Dassault Systèmes Simulia Corporation, 2014.

[23] Foundations and Earth Structures. Naval Facilities Engineering Command. Stovall Street Alexandria, 289 p, 1986.

[24] Pipeline Investigation Report, US Department of transportation. Disponível em http://www.phmsa.dot.gov/pipeline/library/failure-reports, acessado em 21/04/2017 as 08:15.

[25] Dean, R.G. and Dalrymple, R.A. (1991) Water Wave Mechanics for Engineers and Scientists. Advanced Series on Ocean Engineering, 2.

[26] MIYAMOTO, J., Sassa, S. and Sekiguchi, H. (2004): Progressive solidification of a liquefied sand layer during continued wave loading. Geotechnique, vol. 54, No. 10, 617–629.

[27] PINTO, Carlos de Souza, 2000. Curso Básico de Mecânica dos Solos, em 16 Aulas. 1 ed. São Paulo: Oficina de Textos,. 247p.

[28] PINHEIRO, Bianca de Carvalho; LESAGE, J. ; BENSEDDIQ, N. ; PASQUALINO, I. P. . Mesures et modélisation de l'amorçage de l'endommagement par fatigue des tubes d'acier pour le forage et l'exploitation pétrolière. In: Livre des Résumés du 15ème Colloque National de la Recherche dans les IUT, 2009, Villeneuve d'Ascq, França. Institut Universitaire de Technologie A de Lille, 2009

[29] DNVGL-RP-C203 – Fatigue on Offshore Structures. Published by DNVGL on April 1, 2016.

[30] DNVGL-RP-C101 – Design Offshore Steel Structures. Published by DNVGL on February 2011.

[31] Goodman, J., Mechanics Applied to Engineering, Longman, Green & Company, London, 1899

[32] An overview of the Palmgren-Miner rule, 2016. Science Direct. Retrieved from https://www.sciencedirect.com/topics/engineering/palmgren-miner-rule, 14/04/2019.

[33] SHIGLEY, J. E., MISCHKE, C. R., Mechanical Engineering Design. 6 ed. New York, McGraw-Hill, 2001.

[34] PINHEIRO, Bianca de Carvalho, "Avaliação da Fadiga de Dutos de Transporte Submetidos a Danos Mecânicos" COPPE/UFRJ. Masters Degree Thesis. Rio de Janeiro, 2006. Retreived from minerva.ufrj.br.

ANNEX A

Wave data obtention exemple – NOAA Database

```
The data set contained here consists of wave hindcasts done using the
WAVEWATCH III model and GFS analysis winds. The hindcasts cover the entire
globe and are carried out in monthly installments.

There are three types of output -- field output, partitioned data output
and point output.


1.  Field output
    Field output refers to bulk spectral properties over the spatial domain.

    The multi-grid WW3 model is run as a mosaic of grids that are two way
    nested. The spectral parameters are computed on each of these grids and
    are stored in grib 2 format. The naming convention is as follows

      multi_1.[GRIDID].[PARID].[YYYYMM].grb2

    where

       GRIDID are the different grids that make up the WW3 domain. These are
       (in order of resolution)
          glo_30m - The 30 arc-minute global grid
          ao_30m  - The 30 arc minute arctic grid
          ak_10m  - The 10 arc minute regional Alaska grid
                    (it is 15 arc minute along longitude and 10 arc minute
                     along lattitude)
          at_10m  - The 10 arc minute Northern Atlantic regional grid
                    (this grid covers the Gulf of Mexico and out to the
                     continental shelf on the US East Coast. It does not
                     extend across the Atlantic)
          wc_10m  - The 10 arc minute regional grid for teh US West Coast
          ep_10m  - The 10 arc minute grid covering some of the islands in
                    the Pacific (including the Hawaiian islands)
          ak_4m   - The 4 arc minute coastal grid for Alaska
                    (8 arc minute along longituide and 4 arc minute along
                     lattitude)
          at_4m   - The 4 arc minute coastal grid for the US East Coast
                    (includes the waters around the island of Peurto Rico)
          wc_4m   - The 4 arc minute coastal grid for the US West Coast
                    (includes the coastal waters of Hawaii)

       PARID refers to the spectral parameters. The archived parameters are
          wind    - The 10 m wind speeds and direction gtom GFS
          hs      - Significant wave height (in m)
          tp      - Peak period (in s)
          dp      - Average direction at the peak period

       YYYMM refers to the year month in a six digit format

2.  Partitioned data
       WAVEWATCH III separates the 2D wave spectra into partitions by
       identifying the diferent peaks in the spectrum (see manual for details)
       Individual peaks are identified as wind seas or swells using an inverse
       wave age criteria. The file naming scheme is as follows

      multi_1.partition.[GRIDID].[YYYYMM].gz

       These are ascii files that are compressed using gzip. The output in
       each file is as follows

       <yyyymmdd> <hhmmss> <lat> <lon> <name> <nprt> <depth> <uabs> <udir> <cabs> <cdir>
          <partition #> <Hs> <Tp> <Lp> <Theta> <Sp> <Wf>
          repeat for all partitions
       repeat for all times and grid points

       where
          nprt          - Number of partitions
          uabs,udir     - Wind speed and direction
          cabs,cdir     - Current speed and direction
```

```
Hs            - Signficant wave height of partition
Tp            - Peak period of partition
Lp            - Wave length (at Peak period) of partition
Theta         - Mean Wave direction (at Peak period) of partition (in nautical terms)
Sp            - Spectral width of partition
Wf            - Wind sea fraction (portion of partition under influence of wind)
                1 and 0 signify wind seas and swells respectively
```

Partition data is output at every grid point for all grids except the global grid (every other grid point).

3. Point output

Point data is stored at select locations that correspond to either gage data or locations where detailed spectral data was desired. Points can be located in multiple grids in which case the data is extracted from the highest resolution grids. If the point does not lie on a grid location then the data is linearly interpolated from the surrounding grid points. Point data is stored in ascii format but for convenience all the point output files (of a certain type) are tarred together and then gzipped. There are three types of output files

i) WMO format -- (multi_1_base.buoys_wmo*). The file format for individual files is

```
<year> <month> <day> <hour> <uabs> <udir> <Hs> <Tp>
repeat for all times
```

ii) Spectral format -- (multi_1_base.buoys_spec*). 2D spectral data at point location. The file fomat for individual files is

```
<Text string> <Nfr> <Nd> <Np> <Text String>
<fr> (for all frequency bins)
<dir> (for all direction bins)
<yymmdd> <hhmmss>
<Text string> <lat> <lon> <d> <uabs> <udir> <cabs> <cdir>
<E(fr,dir)> (for all frequencies and directions)
repeat for all times
```

where

```
Nfr, Nd, Np       - Number of frequencies, directions and points respectively.
                    (Since a separate file is being generated for each point,
                     Np is set at 1).
fr, dir           - discretized frequency (in Hz) and direction (in radians) bins.
                    Direction is in oceanographic convention.
lat, lon, d       - latitude, longitude and water depth (in m).
E(fr,dir)         - wave spectra in m^2/Hz
```

iii) Bulk parameters -- (multi_1_base.buoys.*). Bulk parameters at point location. The file format got individual files is

```
<yyyymmdd> <hhmmss> <uabs> <udir> <Hs> <H*> <Cp/uabs> <Cm/uabs> Dt
repeat for all times
```

where

```
H*        - Non-dimensional wave height. H* = 3.33*g*Hs/uabs^2
Cp        - Phase speed at peak period
Cm        - Phase speed at average wave period
Dt        - Air sea temperature difference
```